ACTA PALAEONTOLOGICA POLONICA

Isometry in mesosaurs: implications for growth patterns in early amniotes

Type:

Article

Running head:

Isometry in mesosaurs

Abstract:

Mesosaurs were small amphibious tetrapods that lived in western Gondwana during the Early Permian or even earlier, when temperate Permo-Carboniferous conditions were initiated after the glaciations that affected the southern region of Pangea. In this contribution, we applied traditional linear regression morphometrics to analyse proportions of both the skull and limb bones in more than 100 mesosaur specimens. The analyses revealed that all mesosaur bones scale remarkably close to a model of geometrical similarity (isometry), and that this pattern is particularly strong in long bones and also in the skull. These results indicate that juvenile and adult mesosaurs do not display appreciable change in bone proportions, meaning that there are few or no noticeable differences between them during growth. The well-defined isometry, and particularly, the high inter relation between metatarsals and phalanges permit to suggest that the mesosaur hind limb is subject to notable modularity. This evidence strongly argues in favour that the differences previously described to support three mesosaur species in Western Gondwana, might instead reflect natural intraspecific variability, taphonomic features or even possible sexual dimorphism, as recently suggested. Our study also reinforces the general plesiomorphic structure of the mesosaur skeleton, which along with some cranial specializations for ecological fitness and the evidence of
strong isometric growth as we demonstrate herein, may suggest new hypotheses of relationships for mesosaurs which thus, would position them as more basal amniotes than previously thought.

Keywords:

Morphometrics, allometry, Early Permian, Mesosaurus tenuidens, Gondwanan Pangea

Isometry in mesosaurs: implications for growth patterns in early amniotes

Pablo Núñez Demarco[1], Jorge Ferigolo[2], Graciela Piñeiro[3]

[1]**Pablo Núñez Demarco***. Instituto de Ciencias Geológicas, Facultad de Ciencias. Universidad de la República, Montevideo, Uruguay. InGeBa, Facultad de Ciencias Exactas y Naturales -Universidad de Buenos Aires (UBA), Bs.As., Argentina. E-mail: pnunez@fcien.edu.uy

[2]**Jorge Ferigolo**. Seção de Paleontologia, Museu de Ciências Naturais, Secretaria do Meio Ambiente e Infraestrutura do Rio Grande do Sul (SEMA), Rua Salvador França, 1427-90 690-000, Porto Alegre, RS, Brazil. E-mail: jorgeferigolo@gmail.com

[3]**Graciela Piñeiro**. Departamento de Paleontología, Facultad de Ciencias, Iguá 4225. CP. 11400. Montevideo, Uruguay. E-mail: fossil@fcien.edu.uy

Abstract

Mesosaurs were small amphibious tetrapods that lived in western Gondwana during the Early Permian or even earlier, when temperate Permo-Carboniferous conditions initiated after the glaciations that affected the southern region of Pangea. In this contribution, we applied traditional linear regression morphometrics to analyse proportions of both the skull and limb bones in more than 100 mesosaur specimens. The analyses revealed that all mesosaur bones scale remarkably close to a model of geometrical similarity (isometry), and that this pattern is particularly strong in long bones and also in the skull. These results indicate that juvenile and adult mesosaurs do not display appreciable change in bone proportions, meaning that there are few or no

noticeable differences between them during growth. The well-defined isometry, and particularly, the high inter relation between metatarsals and phalanges permit to suggest that the mesosaur hind limb is subject to notable modularity. This evidence strongly argues in favour that the differences previously described to support three mesosaur species in Western Gondwana, might instead reflect natural intraspecific variability, taphonomic features or even possible sexual dimorphism, as recently suggested. Our study also reinforces the general plesiomorphic structure of the mesosaur skeleton, which along with some cranial specializations for ecological fitness and the evidence of strong isometric growth as we demonstrate herein, may suggest new hypotheses of relationships for mesosaurs which thus, would position them as more basal amniotes than previously thought.

Keywords: morphometrics; allometry; Early Permian, *Mesosaurus tenuidens*, Gondwanan Pangea.

Introduction

Mesosaurs have been considered as the oldest known aquatic amniotes (Mac Gregor 1908; Romer 1966; Araújo 1977; Oelofsen 1981; Oelofsen and Araújo 1987; Carroll 1982; Laurin and Reisz, 1995; Modesto 1996, 1999, 2006, 2010; Piñeiro 2002, 2006, 2008; Canoville and Laurin 2010; Piñeiro et al. 2012a-c, 2016; Villamil et al. 2015), but recent morphometric and anatomical studies have suggested that they were more adapted to a semiaquatic life (Nuñez Demarco et al. 2018). They lived in the area occupied by a large and shallow water body at the southwest of Pangea during the Early

Permian (e.g., Santos et al. 2006) or even close to the Carboniferous-Permian transition (e.g., Huene 1940, 1941; Calisto and Piñeiro 2019), spreading through what today are the territories of Namibia, South Africa, south and central Brazil, southeastern Paraguay and northeastern Uruguay (Wegener 1966).

Mesosaurs are of interest to palaeontologists because they might represent the first amniotes that returned to the aquatic environment (Carroll 1988), although they seem to support other hypotheses that suggested that their ancestors also were aquatic or semiaquatic (Romer 1957). Moreover, in a phylogenetic context they were recently found to be the basalmost sauropsids (e.g., Laurin and de Buffrénil 2016; Laurin and Piñeiro 2017, 2018), although other results place them as the basalmost parareptiles (e.g. Modesto 1999; Piñeiro et al. 2012a,b; Tsuji et al. 2012; Modesto et al. 2015; McDougall et al. 2018).

Morphological changes during the ontogeny of a species are often assumed to be adaptive, being modelled by natural selection and by the complex process of growth (Mitteroecker and Bookstein 2007). Divergent selection usually generates phenotypic differences among populations and species, and appendicular synapomorphies related to locomotor adaptations are the frequent targets of studies focusing on the assessment of tetrapod evolution and paleobiology (Bonnan 2004, 2007; Bonnan et al. 2008; Olori 2013).

Mesosaurs provide an interesting opportunity to examine the influence of selection in the developmental and morphological patterns observed through ontogeny. Usually, analyses performed on extinct taxa inherently suffer from difficulties related to completeness, type of preservation and poor taxonomic samples. However, mesosaurs are known from hundreds of complete and articulated individuals and thousands of incomplete and isolated specimens that make them an exceptional case study.

A recent revision of the diagnostic characters that support a taxonomic composition of three taxa within Mesosauridae arrived at the conclusion that only one taxon can be unambiguously recognized, which by priority is *Mesosaurus tenuidens* (Piñeiro et al. 2021).

In this contribution we performed a geometric-morphometric study of cranial and postcranial regions of the mesosaur skeleton, in order to investigate if there are statistically significant morphological differences through ontogenetic development among mesosaurs coming from Brazil, Africa and Uruguay. We also compared our results, mainly for the postcranial region, to the aquatic to semiaquatic reptile *Hovasaurus boulei* from the Permian of Madagascar to test the influence of lifestyle in the construction of the limbs and on the functional patterns of growth. We also discuss the phylogenetic implications of the developmental pattern found in mesosaurs with respect to recent new hypotheses that consider recumbirostran "microsaurs" as basal amniotes (Pardo et al., 2017; Mann et al., 2019, 2020).

Therefore, this paper is organized as follows:

First, we review the basic methodology. The available morphometric data will be presented next: starting with the measurements of the skulls, to investigate the relation of some cranial bones and regions to the postcranium. Subsequently, the internal relationships of the postcranial bones are analysed, ending with comparison of relationships between different bones (with the major focus upon the stylopodia and zeugopodia). We used a traditional morphometric approach with the aim of, *i*) determining whether statistically significant morphological differences occur among mesosaurs, and *ii*) inferring functional and evolutionary implications from the observed patterns. Measurements of the skull, vertebrae and all the limb bones of more than 100 mesosaur specimens were taken, although, our study will concentrate on limb bone

dimensions, as they are often the most and best preserved skeletal elements in the mesosaur fossil record.

Next, the morphology of the mesosaur carpus and its changes observed through the ontogeny were reappraised, followed by an analysis of the ontogenetic transformation of the tarsus in accordance with size, maturity and ossification degree of the different elements.

Subsequently, we focus on the morphometry and relations of the metapodia and phalanges, comparing the results obtained for *Mesosaurus* and the aquatic or semiaquatic Late Permian diapsid *Hovasaurus boulei* from Madagascar. Finally, we will discuss the isometric growth observed during mesosaur ontogeny in a phylogenetic context and in light of recently proposed new hypotheses, which may represent particularly relevant findings to a better understanding of early tetrapod evolution and paleobiology.

2. Materials and methods

We examined a total of 109 mesosaur specimens preserved in different ontogenetic stages, including unborn to young and several very mature individuals.

Specimens revised and analysed in this study belong to six collections, from seven countries:

a) Fossil Vertebrates of the Facultad de Ciencias (FC-DPV), Montevideo, Uruguay;

b) Instituto de Geociências (Palaeontology Sector) of the São Paulo University (GP/2E and PF), São Paulo, Brazil;

c) SEMA, Museu de Ciências Naturais (MCN), Porto Alegre, Brazil;

d) Senckenberg Institute (SMF-R), Frankfurt, Germany;

e) American Museum of Natural History (AMNH), New York, USA;

f) Museum National d'Histoire Naturelle (MNHN) of Paris, France;

g) National Museum of Nature and Science (NSM-PV), Tokyo, Japan;

h) National Earth Science Museum at the Geological Survey of Namibia (GSN-F), Windhoek Namibia.

The available specimens housed in these institutions come from the following lithostratigraphic units: Irati Formation (Brazil), Whitehill Formation (South Africa), Huab Formation (Namibia), and the Mangrullo Formation (Uruguay).

A brief description of the studied specimens and their institutional repositories is provided in Table 1, in the Supplementary Material section.

2.1 Preservation and measurements of the specimens

The studied specimens come from shale and from limestone-dolostone deposits. The specimens from the shale are mostly preserved as external moulds, impressions or casts, whereas permineralized half-buried bones and skeletons come from the limestone and dolostones. 3D measurements from the latter could not be taken accurately, because this preservation does not allow removal of the bones from the matrix without damaging them. Long bones are mainly elliptical in their mid-diaphyseal cross section (the femur is somewhat triangular) and are almost always resting in similar positions with the long axis parallel to the sedimentary layers, even if the specimen is resting in lateral view. Therefore, 2D measurements are a good approximation to the real dimensions and the maximum length and width can be obtained confidently.

Mesosaur specimens were photographed, and 2D measurements were taken using the digital images, with an error of 0.1 mm. The selected specimens are articulated or semi-articulated skeletons in which the anatomical position of the bones was known, or could be determined.

Our study focuses mainly on the postcranial region of *Mesosaurus tenuidens*, because a considerable number of specimens preserving the skull are severely damaged; despite this, we could obtain reliable statistical results by measuring 26 mesosaur skulls. The skull length from the tip of the snout to the posterior edge of the postparietals, the skull maximum width, the snout length from the tip of the snout to the orbit, the snout width, and the length between the posterior border of orbit and the posterior border of the skull were measured. Moreover, we compared the skull length in relation to the growth of some postcranial bones through different ontogenetic stages, and these measures were compared with the mean of the centrum length along the available vertebrae in each specimen. The mean centrum length was calculated for the neck, trunk, and tail regions and also for the entire body (data and measurements for analyses of centrum length patterns were provided in Nuñez Demarco et al. 2018). Knowing the total number of vertebrae of mesosaurs (~101) and multiplying it by the mean centrum length, it is possible to estimate the total length of the specimens. Nuñez Demarco et al. (2018) showed that this calculation is more accurate if the mean centrum length is used instead of the length of one specific vertebra or vertebral segment (e.g. sacral vertebrae).

In the postcranial region, measurements of the appendicular skeleton were prioritized, as these bones are well represented, both in articulated specimens and as isolated elements, thus guaranteeing a good sample size for statistical tests.

Total length was measured in all long bones (humerus, radius, ulna, femur, tibia, fibula, metacarpals, metatarsals, and phalanges, see Fig. 1). Maximum diameter of the

proximal and distal bone ends (epiphyses are mostly cartilaginous) and minimum midshaft (diaphysis) diameter were measured for the humerus, radius, ulna, femur, tibia and fibula. Only the diameter of the first metatarsal proximal epiphysis (mostly ossified) was measured. Disarticulated phalanges that could not be assigned to a specific toe were excluded.

Additionally, astragalus length and width in its proximal, central and distal regions, and calcaneum length and width in its central portion, were measured (length was measured from the anterior point of the bone to its most posterior point).

Measured regions are indicated in the corresponding figures. Elements from both sides of the body (when available), were measured to provide better sample sizes for the analyses. Therefore, in some of the performed test some individuals may be represented by two sampled points. To avoid any confusion, the number of samples and the number of individuals sampled was indicated in every analysis.

Anatomical identification of the limb bones at the zeugopodial region is difficult to assess if they are preserved in isolation, since radius and ulna can be mistaken for metapodials of larger specimens (Fig. 1).

To complete the morphometric study and for comparative purposes, we also analyzed 30 articulated specimens of *Hovasaurus boulei* preserving the hind limbs. *Hovasaurus boulei* is an early diapsid from the Upper Permian sequences of south-western Madagascar (Currie 1981; Carroll 1981, 1982; Caldwell 1994, 2002) which possesses similar aquatic adaptations to mesosaurs, except for development of pachyosteosclerotic ribs in the latter. *Hovasaurus* is known from a large number of articulated and almost complete skeletons with very good preservation of the hind limb components, which allowed Caldwell (1994, 2002) to study the ossification patterns of this taxon through the ontogeny. Limb measurements for 30 specimens of *Hovasaurus*

boulei were taken from drawings of Currie (1981) and Carroll (1981) and from photographs of the specimens deposited in the collection of the MNHN of Paris taken by a colleague of our research group (see Fig. 2).

2.2 Allometric equation

Changes between parts of an organism and their proportions are generally described by the allometric equation (Snell 1892; Huxley 1924), given by a power law formula:

1) $y = b\,x^{a}$

where y and x are variables that express the dimension of some parts or components, b is a constant, and a is the law's exponent, or in this case, the allometric coefficient. This equation implies that change in one quantity (x) results in a proportional relative change in another (y). This expression can be easily simplified applying a logarithmic transformation to get:

2) $\log(y) = \log(x)\,a + \log(b)$

This last expression has the advantage of being a line with slope equal to a, but using the original variables on a logarithmic scale. Thus, the coefficient a reflects the intensity of differential growth between the different parts. This coefficient can be determined by a linear regression of the variables x and y.

More precisely, bivariate relationships are identified as isometric if the 95% confidence interval of the slope of equation (2), includes 1 (e.g. Rubenstein 1971; Leduc 1987; Anderson et al. 2016). If $a > 1$, then y grows faster than x (positive allometry) and if $a > 1$, x grows faster than y (negative allometry). Meanwhile, a non-linear relationship between the two variables may imply changes in the growth rate during ontogeny.

Despite the apparent simplicity of the method, it requires some cautions and considerations as follows:

i) For the linear adjustment to be valid there must be a good or strong correlation between the two variables. Usually, correlations with r-squared values higher than 0.70, are considered strong and reliable.

ii) The regression method to define a line of best fit between *x* and *y*, also should be considered carefully. Two methods are usually considered; the ordinary least squares (OLS) and the reduced major axis (RMA). The last one is also known as the standardized major axis (MA) or the geometric mean regression (GM). OLS assumes that *x* is the independent measurement known without error, and all error is attributed to the *y* variable, being the dependent measurement –or error in *y*- very much higher than error in *x*. Instead, RMA assumes that both, *x* and *y* were measured with error, but, above all, RMA is symmetric, meaning that the slope of the regression of *x* on *y* and of *y* on *x* are the same. Meanwhile, OLS is asymmetric, meaning that the result will change depending on which variable is identified as *x* and which as *y* (Smith 2009). In morphometric analyses, both variables commonly have measurement errors, usually the same error. Although this error can be minimized, there is an unknown noise introduced by taphonomy, which is always an important factor in palaeontology. Moreover, as we are trying to calculate allometric relationships – a mutual, co-dependent law underlying *x* and *y* relationship-, the selection of which variable will be on the *x* axis and which on the *y* axis is arbitrary. Additionally, we have to pursue a solution with a symmetric interpretation capable of predicting cases that fall outside of the domain of the regression. In such conditions, RMA is recommended (Leduc 1987; Ricker 1973; Bonnan et al. 2008; Smith 2009). In this work, RMA curves were calculated using the Matlab program developed by Trujillo-Ortiz and Hernandez-Walls (2010). The

confidence intervals were calculated using both Ricker (1973) and Jolicoeur and Mosimann (1968) and McArdle (1988) procedures available in the same program. As the results are practically similar, we show only the later one in the plots.

iii) Another issue is the log transformation of the data. As previously shown, logarithm is applied to the data to solve equation (1) and to calculate *a* coefficient. However, logarithm is commonly applied in biological sciences to normalize the data, to reduce the skewness of the distribution and to reduce variability, especially data that include outlying observations (Zar 1999; Feng et al. 2014). Normalization is also a necessary condition for OLS and RMA. However, as Feng et al. (2014) have demonstrated, if the data already have a normal distribution, the log transformation can produce a non-normal distribution and even increased variability. In our case, the mesosaur data have a normal distribution and then log-transformation is not recommended. To solve this contradiction, we applied the procedure two times. Firstly, we log-transformed data in order to calculate coefficient *a*. If the data satisfy the condition that the 95% confidence interval includes 1, then the growth is isometric, and the allometric equation becomes:

3) $y = bx + c$

where *b* is the slope of the curve, *c* is a constant and both *x* and *y* grow at the same rate (isometry). Thus, we recalculated the linear adjustment of the data without log-transformation of the data, in order to establish a more reliable relationship between the variables. All the linear plots presented in this work use non-logarithmic data, following eq (3), but each plot is linked to the values of the constant *a* calculated with logarithmic data. This also has the advantage that data and plots can be directly analyzed and interpreted (Feng et al. 2014).

iv) Finally, we must be able to ensure that the sampling distribution is statistically significant; something that is not easy in palaeontology. In our case we can assume that 1) the sampled mesosaurs are a random and representative sample of the population. This is strengthened by the fact that we studied samples collected throughout the Irati, Mangrullo and Whitehill formations, at different levels and lithologies, and that were collected by different people. 2) All the mesosaurs are likely to be representative cross-section of the mesosaur population. Different sizes and ontogenetic stages have been already recognized in most of the studied samples (Piñeiro et al. 2016, Piñeiro et al. 2021), so it can be assured that various groups of different ages are represented. 3) Bone dimensions correctly represent the actual dimensions of the mesosaurs from which they derived.

As in similar works (e.g. Bonnan 2004, 2007, Bonnan et al. 2008; Olori 2013), we plotted bone length against bone width to obtain allometric profiles for each bone. In addition, we compared different bone measurements to observe their allometric relationships. In other words, bivariate relationships between intra- and inter-bone dimensions were examined. Further, we compared the results with data provided by the studied *Hovasaurus* specimens, in order to observe similarities and differences.

It is important to clarify that most of the appendicular mesosaur elements display a simple morphology with few discernible landmarks making them unsuitable for a geometric morphometric study. A notable exception is the humerus of the mesosaurs. However, such analysis is beyond the scope of the present study and will constitute a separate contribution.

To test our allometry results and verify that these are not simply the result of the chosen samples, the data were resampled uniformly at random, with replacement, 100,000 times (e.g. Kowalewski and Novack-Gottshall 2010). The result of each

resampling was analyzed and compared with the original result (for log transformed data), as well as the average result of the resampling. This bootstrap method is particularly important to know how much the sample statistic varies, and to assess the uncertainty surrounding it.

3. Results

3.1. Isometry

Linear adjustments made with log transformed data show that mesosaurs display a strong correlation and isometry (Figs 3 to 10). This kind of growth is observed in the skull and also in the postcranial region, particularly marked at the vertebral column, and at the fore and hind limbs (See also Table 1).

3.1.1. The isometry of the mesosaur skull

Figure 3 (A-F) summarizes the relationships between different dimensions of thirty-nine mesosaur skulls and the statistical parameters of the analysis. Skull length and snout length (Fig. 3B) have an isometric relationship with the most intense correlation. This is probably because the snout length is a substantial part of the skull length. Curiously, when the quantity “skull length minus snout length” is plotted against skull length, the relation is also isometric (Fig. 3B, square dots). Moreover, all the dimensions measured have isometric slopes (Fig. 3G), the only exception is when comparing the skull length and the orbit length (Fig. 3C) where the 95% interval did not include 1, although the value is remarkably close to 1. The relationship in this case presents a slight negative

allometry. The back of the skull and the orbits are among the elements that display the greatest taphonomic deformation due to compaction during diagenesis. Therefore, it is expected that these elements exhibit greater noise and a lower correlation as it can be seen in Fig. 3C, D, and H. Curiously, the orbit length vs. the maximum width of the skull have an isometric relationship (Fig. 3F), possibly because both elements were uniformly distorted. If orbits and snout are not deformed equally during compaction, that could explain the low correlation and lack of isometry between the length of both the skull and the orbit (Fig. 3C). The bootstrap analysis reinforces these results (Table 1). Moreover, all the parameters including skull length and the orbit length include 1 in their confidence intervals, and therefore they can be considered isometric. However, skull length and the orbit length display great variability. For example, for these particular variables, only 41% of the 100,000 re-samples do include the number 1 in their 95% interval. This result does not change the fact that the average result of the resampling and its confidence interval do include 1, but reflects a higher uncertainty level among these measurements, probably related to taphonomic artifacts as mentioned earlier.

3.1.2. *Isometry of the postcranial bones*

The relationship between the length and width of the different long bones in mesosaurs has a correlation coefficient higher than 0.7 and gives values of coefficient *a* close to 1. Figure 4 summarizes all the statistical intra-bone relationships of the measured bones, calculated using logarithmic data (equation 2). All the 95% confidence intervals included 1, except for the astragalus, although it is still very close to 1 (Fig 4A). This is not unexpected given that this bone has a more delayed ossification process (including a

late fusion with the navicular) which can be observed along its growth (Piñeiro et al. 2016). Figures 5 and 6, show the linear plots (according to equation 3) for stylopodium and zeugopodium of forelimbs and hind limbs respectively; these figures also show these regions measured in each bone. The resampling statistics emphasize the previous results (Table 1). All the resampling means have values closer to 1 with confidence intervals that include 1. Even the mean correlation coefficient of nearly all the resamples is greater than to 0.7 (the only exception being tibia length vs tibia distal width). Moreover, the length:width relationship for each bone in more than 90% of the 100,000 re-samples does include 1 in its 95% interval. This implies than there is a strong regularity among the data, and that the results do not depend on specific specimens. The only exception is the astragalus, that shows greater variability.

The relationship between the length of different bones in *Mesosaurus* has also a high correlation (> 0.8), with values of the coefficient very close to 1 and their 95% confidence intervals including 1. That implies that there is a strong isometry in mesosaurs between all these structural elements.

Figure 7 summarizes all the statistical intra-bone relationships (slope *a*, correlation, and number of samples) of the measured bones, calculated using logarithmic data (equation 2). Resampling corroborates and reinforces these results (Table 1). All the mean slopes in the analysis are close to 1 with the confidence interval including 1, which indicates isometry. Most of the measurements show great homogeneity, since most of the resamples (more than 90%) resulted in isometry. Some measurements also show some variability, such as the femur:tibia, femur:fibula, humerus:ulna, humerus:radius and humerus:metacarpals III, IV and V ratios. This may indicate more intraspecific variability, or greater variation due to taphonomy in these elements. In particular, it should be noted that there are comparatively fewer

measurements in the forelimbs, because the preservation of these elements in good condition is rarer.

The linear relationship between the length of the measured mesosaur humeri vs. metacarpals is shown in Fig. 8A and femora vs. metatarsals in Fig. 8B. The relation of the length of the femur vs. humerus (Fig. 8C) and humerus vs. ulna and fibula (Fig. 8D) were also calculated. In all these cases, an isometric relationship can be observed (see also Fig. 7). The length of the tibia and fibula was also compared against the length of the femur (Fig. 9). In general, information coming from the forelimbs is less available than that of the hindlimbs; often due to taphonomic biases in which the forelimbs tend to be preserved under the body. However, despite metacarpal data are notoriously scarcer than those from metatarsals (Fig. 8A, B), an isometric relationship can be observed.

In mesosaurs, the radius and the ulna are, on average, the same length. The same occurs with the tibia and the fibula. Likewise, radius and ulna are slightly shorter than tibia and fibula. In general, zeugopodium length tends to be 60% of the stylopodium, maintaining a strong isometric correlation between them (Fig. 7). For comparison, in *Hovasaurus*, the tibia tends to be from one to three millimetres longer than the fibula, while tibia and fibula lengths are on average 80% of the femur length, also maintaining a strong correlation between them. Moreover, in *Hovasaurus* the ulna and radius are on average 50-65% of the humerus length, following an allometric ontogenetic relationship (Currie 1981).

Hind limb proportions (e.g., hindlimb length excluding the autopodium) and the length of the pes have been found to be particularly useful in identifying species ecology as well as for species characterization (Nuñez Demarco et al. 2018, Farlow et al. 2018). Consequently, we analysed the relationship between stylopodium plus

zeugopodium against metapodium (Table 1). The relationship between femur plus tibia against metatarsal i (and metatarsal v) also shows strong isometry. However, the relationship between humerus plus radius against metacarpal i (and metacarpal v) presents negative allometry. This result would not be strange considering that it is similar to the pattern observed in extant species (Farlow et al. 2018). However, it is not clear whether this pattern in mesosaurs is related to the small number of samples analysed or not. As will be seen later in section 3.5, phalangeal lengths of mesosaurs are strongly correlated with the metapodia length, consequently, the relationships obtained with the metapodia will remain almost unchanged when considering the autopodia. Therefore, the evidence indicates that mesosaurs possess a strong isometry in their hindlimbs and isometry or some level of negative allometry in their forelimbs.

The relationship between mean vertebral length and skull size also follows a linear relationship (Fig. 10A, Table 1). The correlation and parameter *a* and its 95% interval are 0.98±0.2, with a correlation coefficient of 0.91 (in logarithmic and in non-logarithmic scales). When comparing the skull length to the femur length (Fig. 10B, Table 1), and the skull length with the stylopodium length (Fig. 10C, Table 1), an isometric linear relationship is seen again. Moreover, previous studies have shown that skull length vs. neck length, and skull length vs. mean tooth length are also isometric among mesosaurs (Piñeiro et al. 2021).

3.2. The *Mesosaurus* carpus

Interpretation of the anatomical construction of the bones in the mesosaur manus is a collateral result of this research. Historically, the carpus structure has been subjected to very different interpretations. For instance, Gervais (1865) described the presence of

only two bones in the proximal series of *Mesosaurus tenuidens*, assuming that there is a small radiale and a large cubitale (ulnare). The pisiform was thought to be absent in the type specimen described by Gervais (1865), and only four distal carpals were suggested to be preserved.

Two proximal carpal elements without perforation between them were also described by Huene (1941) for *Mesosaurus tenuidens*, identifying such elements as the ulnare and the intermedium. Moreover, Huene (1941) also described four distal tarsals for *Mesosaurus* the first one being the largest. The same anatomical arrangement was proposed by Kuhn (1969), but for this author, the perforating foramen between the bones was present.

According to Seeley (1892), the carpus in mesosaurs is instead distinguished by the presence of three bones in the proximal series and four small elements in the distal line. Curiously, the intermedium is identified as the lunar by Seeley (1892) and the ulnare and the lateral centrale as the cuneiform and scaphoid (or centrale), respectively. However, Seeley (1892) argued that there is no definitive evidence to identify a scaphoid in the mesosaur manus, but he suggested that the structure of the mesosaur carpus is reminiscent of that present in the mammalian type if the scaphoid and the pisiforme are unossified in the radiale and ulnare positions, respectively. Seeley (1892) also emphasized that the four bones in the distal line are anatomically equivalent to the trapezium, trapezoid, magnum and unciform, the first being the smallest and the fourth the largest.

Mac Gregor (1908) stated that close to the intermedium there is an ossified radiale in *Mesosaurus*, which is the largest element in the proximal series. However, he surely misidentified this large bone, which may have been the first distal carpal. The ulnare is also present and delimits a small passage for a blood vessel along with the

intermedium. Four tarsal bones comprise the distal series, and the first one is the largest. More recently, Modesto (1996, 1999, 2010) suggested that there could be a different structure in the carpus of *Mesosaurus* Gervais, 1865 and *Stereosternum* Cope, 1885a. According to Modesto (1996, 1999, 2010) the carpus is formed by nine ossified elements in the latter taxon, the intermedium, the ulnare, and the lateral centrale in the proximal series and a spindle-shaped perforating foramen is present between the first two; five tarsals comprise the distal series. The radiale remains unossified and the medial centrale could have been also unossified or it is absent. Modesto (1996, 2010) stated that a small pisiforme characterizes the carpus of *Stereosternum*, as he did not find this bone in *Mesosaurus*. Moreover, *Mesosaurus* would also be differentiated from *Stereosternun* by fusion of the intermedium and the lateral centrale; thus, just two bones occur in the proximal carpal series (intermedium+ulnare).

A recent study (Piñeiro et al. 2021) showed that *Stereosternum tumidum* is a junior synonym of *Mesosaurus tenuidens*, and thus the differences found by Modesto (1996, 1999, 2010) are taphonomic or possibly influenced by the ontogenetic stage of the specimens that he analyzed. Moreover, other studies (e.g., Rossmann 2000) found no differences between the *Mesosaurus* and *Stereosternum* carpus, as they both possess two proximal bones and five elements in the distal series, but doubts remain if a lateral central is present in the latter. However, according to Rossmann (2000), *Brazilosaurus sanpauloensis* Shikama and Ozaki, 1966 would have had a different carpal structure consisting of three proximal elements and only four distal tarsal bones.

On the other hand, *Brazilosaurus sanpauloensis* was recently found to be also a junior synonym of *Mesosaurus tenuidens* (Piñeiro et al. 2021) and the specimen that was considered the holotype for this species was reinterpreted as a subadult or young adult individual based on the poor development of the three featureless bones in the

proximal series of the carpus and by the presence of only four distal carpals (see also Piñeiro et al. 2016).

It is important to note that the mesosaur manus is only well-preserved in a few of the analyzed specimens. In this study, which considers juvenile and adult individuals of *Mesosaurus tenuidens* to comprise the only valid mesosaur species, we suggest that an ulnare and an intermedium are well ossified and always present bones in the proximal line of the mesosaur carpus, and an irregularly or well-shaped perforating foramen for blood vessel passage, is present between them in adults or subadults (Figs. 1B, 11 and 12). A third large bone occupying a more medial position in the proximal carpal series is thought to be the lateral centrale, which probably includes also the medial centrale fused very early in the development. We have evidence supporting this last hypothesis in one immature individual which shows a probable medial centrale close to the lateral centrale (Fig. 11B). The radiale is identified as an isolated small bone positioned medial to the lateral centrale in just a few specimens that were preserved in early stages of development (Figs. 11B and 12B, C_1, C_2). We have enough evidence to hypothesize that the radiale fuses to the lateral centrale, because it appears isolated close to this last bone and approaches to it, until becoming fused (Fig. 12B, C_1, C_2). However, is worth noting that the radiale is not observed in very young specimens, and it is rarely preserved in its original anatomical position in adult individuals.

Four or five bones can be seen in the distal carpal series of subadult and adult individuals, a feature also observed for the tarsus in previous studies (e.g., Piñeiro et al. 2016; Piñeiro et al. 2021). There is also considerable variability in the degree of ossification and size of each of these distal carpal bones, although the fifth, when ossified, can be the smallest of the series in adult specimens, and the first or the fourth are the largest. Such a size pattern for the first and fourth distal carpals could simply be

individual variability, taking into account that the fourth can be large in one manus and normally small in the other (Fig. 11 D_1, D_2). Even though, the largest bone in the distal carpal series of synapsids and basal sauropsids is commonly the fourth one and the fifth is the smallest.

Moreover, another very small element is present in the mesosaur carpus, although it is only rarely preserved along the other carpal bones. Regarding its position lateral to the ulnare, this small bone may be the pisiforme (Fig. 11C_2, D_1; and 12D, E_2), but as shown, it can be preserved in the right manus but absent in the left one of the same individual, or vice-versa. A small pisifome may also occur in the type specimen of *Mesosaurus tenuidens* (Fig. 11D_1-D_2) but partial degradation of the skeleton by the action of scavenger organisms such as pygocephalomorph crustaceans, could have removed some of the smallest bones. It has been suggested that the pisiforme is a sesamoid bone (see Fabrezi et al. 2007), and if so, its appearance or its absence (even in the manus of the same individual) could depend on taphonomic processes. For instance, some small elements positioned laterally to the lateral centrale are misidentified as the pisiforme (see Bickelmann and Tsuji, 2018) but they are not preserved in the anatomical position of this bone. Thus, these small elements could be instead interpreted as sesamoid bones. We should note, though, that the pisiforme is so small that it can be easily lost or removed from its original position during the fossilization process, thus explaining why we have found this bone in just a few (fewer than five) of the studied specimens.

As can be seen from Table 2, the anatomical construction of the carpus has been differently interpreted by previous authors, denoting strong subjectivity in their conclusions that is related mostly to taphonomic artifacts, but that also depends on the grade of maturity of the studied individuals. Therefore, establishing the identity of the

bones present in the carpus, as well as in the tarsus, will depend on the degree of ossification and fusion of the elements through the ontogeny. Even the fusion of the intermedium with the lateral centrale, suggested as a diagnostic character for *Mesosaurus* (e.g., Modesto 1996, 2010), is the last stage of the ontogenetic process that is characterized by the presence of only two bones in the proximal carpal series (intermedium and ulnare) (see Table II).

On the other hand, condensation and ossification of the fifth distal carpal and distal tarsal bones may be independent of the process of condensation and ossification of the digital arch (Shubin and Alberch 1986), and so the differentiation of this toe can be achieved indistinctly earlier or later in the ontogeny.

Therefore, based on the new evidence, we can summarize the structure of the mesosaur proximal carpus as being formed by three or four bones in the juvenile stage (intermedium, ulnare and radiale plus fused medial and lateral centralia), and only two in adults, the intermedium (fused to the lateral centrale+radiale+?medial centrale complex) and the ulnare. Concerning the distal series, there can be four or five bones as also occurs in the tarsus, the fifth being the last one to ossify. As a result, the distal carpal or tarsal V is always the smallest of the series.

3.3. Mesosaur tarsus and ontogenesis

Ossification of the tarsal elements also correlates with the ontogenetic stage of the individuals (Piñeiro et al. 2016). Figure 13 displays the ontogenetic stage of several mesosaur specimens. Specimens A, D-I, K, O-S were previously analyzed by Piñeiro et al. (2016), whereas, specimens B, C, J, L, M, N, T are included in this work. In general, ontogenetic stages have a good correlation with size. Only specimens “G” and “L”

appear to be respectively more or less ossified than the surrounding specimens. Figs. 9 and 10A show the tarsal elements of the studied specimens listed in Fig. 13.

Six groups (ontogenetic stages) can be clearly identified:

(*i*) The foetal stage being represented by only one individual with tarsal elements not yet ossified, and a femur length less than 10 mm (Fig. 9, specimen A, see also Piñeiro et al. 2012a; 2016).

(*ii*): A second stage of young individuals with femur less than 22 mm long, which show no tarsal elements or an incipient ossification of the astragalus (e.g., A-D). This group can include the previous one.

(*iii*): A third group characterized by individuals with femur lengths between 22 to 28 mm showing tarsal elements beginning to ossify, with barely ossified and rounded (featureless) astragalus and calcaneus and absence of distal tarsals (e.g., E-J) -or in a very incipient state of ossification (e.g., G in Fig. 9)-. The astragalus and calcaneum remain separated and the foramen for the perforating artery is not visible (see Piñeiro et al. 2016).

(*iv*): The fourth stage comprises mesosaurs with femora longer than 28 mm and shorter than ~40 mm, which have well ossified tarsal elements consisting of a square astragalus and triangular calcaneum, an incipient foramen for the perforating artery and a rounded and immature navicular (fussed centralia 1 and 2). Note that this group has specimens with the astragalus well ossified and perfectly showing the distal border with centralia 1 and 2 not yet completely coosified (e.g., specimen N). The first four distal tarsals can be either immature (e.g., L, N) or well-developed (e.g., K, O). Meanwhile the fifth distal tarsal appears to be absent.

(*v*): The fifth group is composed by mesosaurs with femora of ~40 mm long, characterized by well ossified tarsal elements, a conspicuous foramen for the perforating

artery and a well-developed navicular (fused centralia 1 and 2) in an elongated form -but still not fused to the astragalus- (e.g., P, Q).

(*vi*): Finally, the sixth group, composed by mesosaurs with a femur length greater than ~40 mm long, where the tarsal elements such as the astragalus and navicular become fused (e.g., R, S, T). The fifth distal tarsal is present either immature (R) or well developed (S).

While ossification of the astragalus, navicular and calcaneum appears to correlate well with size, ossification of the distal tarsals does not correlate so well. Indeed, distal tarsal ossification appears to be very variable. For example, specimen G in the stage iii, includes four well-developed distal tarsals, and even a bone that appears to be an incipient navicular (fused centralia). Among mesosaurs with femur length between 23 and 40 mm, some specimens show incipient ossification of the distal tarsals (e.g., L, N) while others display an advanced degree of ossification (e.g., K, O). Moreover, among mesosaurs with femurs greater than 40 mm, some specimens can have the fifth distal tarsal poorly developed (e.g., Q, R, T) whereas in others the fifth distal tarsal is instead well developed (e.g., P, S) (see also Piñeiro et al. 2021). Therefore, we can say that the presence of the fifth distal tarsal appears to be characteristic of the most mature mesosaurs (e.g., P-T).

Figure 14 summarizes the six ontogenetic (tarsal) stages and its correlation with size, as well as tabulates the approximate dimensions of the various bones in those stages, supported by current observations. Based on the ontogenetic series and the lack of ossification of the carpal and tarsal elements, stages *i* to *iii* correspond to juvenile individuals, stage *iv* is presumed to characterize sub-adults, and the stages *v* and *vi* the "elder" adult phase (see also Piñeiro et al. 2016).

3.4. Metapodial relationships in *Mesosaurus* and *Hovasaurus*

The relationship between metacarpals and metatarsals of each manus and pes in both *Mesosaurus* and *Hovasaurus* is addressed in Fig. 15. For each finger and toe we plotted metapodium length versus the metapodium position, where each measured hand or foot is represented by a curve in the graph.

Curiously, mesosaur metacarpals have very varied patterns (Figs. 1, 15A). In most mesosaur specimens, the size of the metacarpals increases from the first to the second and then remains about the same size for the third and fifth metacarpals being the fifth, the longest. However, some mesosaurs show a maximum in the third metacarpal and a decrease in size in the fifth metacarpal, while an almost constant length in all metacarpals is seen in one specimen.

Hovasaurus has a more regular pattern, with metacarpal III or IV being the longest, with lengths thus decreasing in size towards metacarpals I and V (Figs. 2, 15B).

In contrast, a characteristic mesosaur feature is that the metatarsals of each toe become successively longer from digit to digit, with the first metatarsal being the shortest and the fifth the longest (Figs. 1, 15C). The second metatarsal is approximately 1.25 (1+1/4) times longer than the first, whereas the third is 1.5 (1 + 2/4) times longer, the fourth one is 1.75 (1+3/4) times longer and the fifth one is approximately 2 times longer than the first metatarsal. The empirical proportion followed for the mesosaur metatarsals is: mt(n)=mt(1)+n/4, where mt(n) is the measure of the first metatarsal and mt(i) is the measure of metatarsal n. In *Hovasaurus* (Figs. 2, 15D) the second metatarsal is 1.7 times longer than the first one, the third metatarsal is 2 times longer, the fourth is 2.1 times longer, but the fifth one is only 1.66 times longer than the first metatarsal.

3.5. Phalangeal relationships in *Mesosaurus* and *Hovasaurus*

The phalangeal formula of the manus and pes in *Mesosaurus* is 2-3-4-5-3 and 2-3-4-5-5 (digit I to digit V, including the vestigial clawed tips), respectively (see Fig. 1). The claw of the fifth toe is only observable in three out of 78 specimens that preserve the phalanges. An unusual but diagnostic character of mesosaurs is that digit V is the longest of all, decreasing regularly to digit I (Fig. 1).

As in previous analyses, we examined the phalanx size variation within each finger and toe. For each finger/toe we plotted toe length versus its phalangeal position, and each measured finger/toe is represented by a curve in the graph (Figs. 16, 17, 18). In mesosaurs, the phalanx length decreases successively from proximal to distal, following the same general constant relationship in each finger/toe. The relationship is empirically approximated as 1/(n+1) (or more precisely: 1/[1.2(n+1)]) meaning that, the length of the first phalanx (n=1) is 1/2 of the respective metapodial length, the second phalanx is 1/3 of the metapodial length, the fourth phalanx is 1/4, and the fifth phalanx (including the clawed tip) is 1/5. Normalizing the results by the metapodium length allows comparison of all the fingers measured in 18 and toes measured in 43 different individuals, following the same general pattern (Figs. 16F, 17F). Although some minor variations over this pattern can be clearly observed, phalanx length differs less than 2 mm from the population mean or empirical values (Figs. 16F, 17F). It is worth noting that these phalanx-metapodium relationships do not change within the mesosaur population; thus, it is independent of size or age. This relationship persists on both feet and hands, and each of the five fingers/toes of each specimen follows the same pattern. Even considering that natural intraspecific variation or taphonomical distortion of the bones occur, such geometrical regularity is outstanding.

On the other hand, *Hovasaurus boulei* has a phalangeal formula of the manus as 2-3-4-5-4 and 2-3-4-5-4 for the pes (Currie 1981). The comparative analysis performed revealed that unlike *Mesosaurus*, *Hovasaurus* IV toe is the longest, as is usual in basal Permian tetrapods (Romer 1956). The variation found in the *Hovasaurus* phalanx size within each finger is plotted in Fig. 16 and that for each toe is plotted in Fig. 18.

Phalanx size of the *Hovasaurus* manus is plotted in Fig. 17G-L. Digit I of the first phalanx is slightly longer than the respective metacarpal, while the second phalanx represents approximately 80% of the respective metacarpal (Fig. 17G). Digits II, III and V have the first and second phalanx of approximately the same size (~60-70% of the metatarsal). In digits II and V, the third phalanx decreases again in length, whereas in digit III the third phalanx increases in length in most specimens (Fig. 17H-I). Digit IV has the first and fourth phalanx of approximately the same size, ~70% of the respective metacarpal, whereas the second and third phalanx also are about the same size but are shorter than the first and fourth (~60% of the metacarpal).

Regarding the pes, the plotted toe phalanges decrease successively in size (Fig. 18), although the *Hovasaurus* toes show three distinct patterns. Digits II, III and V display a similar pattern (which cannot be given in a simple formula as in mesosaurs). The first phalanx is approximately 50% the length of the respective metatarsal, the second phalanx is ~40% the length of the metatarsal, the remaining phalanges are ~35%, ~30% and ~28% the length of their metatarsals, respectively. This produces a pattern that follows a concave up curve. However, digit V differs in that the first phalanx is 80% the size of the metatarsal and the remaining phalanges follow the proportions ~50%, ~45%, and ~30% (Fig. 18E). Furthermore, the digit I has different proportions; the first phalanx is ~90% the length of the respective metatarsal, whereas

the second phalanx is ~60% of the metatarsal, following a somewhat concave pattern (Fig. 18A).

Both the manus and pes patterns in *Hovasaurus* reveal great variability. The phalanges not only decrease in size as in *Mesosaurus*, they also maintain the size of the previous phalanges or metapodium and even increase in size with respect to the previous one. Moreover, each finger/toe has a different pattern, particularly digits I and V. Even though the pattern of the hands and feet seems to be similar, they also show notable differences. This condition in *Hovasaurus* is in complete contrast to the strongly regular pattern observed in *Mesosaurus*.

From another point of view, Figs. 19 and 20 show respectively the available data for toes in *Mesosaurus* and *Hovasaurus* arranged in stacked bar diagrams and sorted by size. Unlike the previous diagrams that show the morphometric relationships, these diagrams allow better appreciation of the taphonomic state of the samples and the size distribution within the species. Most of the mesosaur specimens have their phalanges preserved (Fig. 19), the first toe being the best preserved and the fifth one the worst. *Hovasaurus*, instead, has a more homogeneous preservation of toes (Fig. 20).

As previously shown, mesosaur bones follow an isometric relationship and size has a good correlation with ontogenesis (Fig. 9), therefore, the size sorting of the samples can be related to the ontogenetic growth pattern of the species. Whereas continuous growth is observed in mesosaurs, which does not appear to stagnate (Fig. 19), the length of the metatarsals in *Hovasaurus* seems stuck in larger individuals (Fig. 20), perhaps reflecting a limit of growth. Additionally, *Hovasaurus* has a good representation of the ‘juvenile’ population (with metatarsals less than 10 mm) and of larger specimens that may represent the ‘adult’ population (with metatarsals longer than 10 mm). In mesosaurs, a more continuous and gradual pattern is observed, although a

slight jump can be seen after the leftmost individual in Figure 19 (the unborn mesosaur specimen, FC-DPV 2504, Piñeiro et al. 2012a). This jump, also visible in the other metatarsals, indicates the lack of information in the transition between the foetal state and the youngest specimens recorded. This result is to be expected because according to information from extant reptile groups, the neonate stage is presumably fast (see Figs. 13, 14).

4. Discussion

4.1. Isometry, size and maturity

Isometric growth is suggested as an ancestral feature in the development of early tetrapods (Olori 2013). The strong isometry and correlation observed between most of the mesosaur bones even allows reconstruction of the skeleton by only knowing the size of a single bone, as long as it can be correctly identified, with the exception of the scapulocoracoid and the ribs (see Piñeiro et al. 2021). Moreover, according to the present study, mesosaurs can be now classified ontogenetically by the size of their bones, which correlate with the grade of ossification of their carpal and tarsal bones (Piñeiro et al. 2016).

Further, isometric growth means that all body parts increase at the same rate and the juvenile proportions are not different from those of the adults. Although there is some natural variability in mesosaurs, it is limited. There are no particular specimens that exhibit great variation from others. However, regions or bones that display more variability than others can be identified, and we assume that they are subject to taphonomic features or ontogenetic variability. For example, the distal ends of the

appendicular bones ossify late depending on age and possibly even denoting sexual differences (Bonnan et al. 2008, Piñeiro et al. 2021), so, it is not surprising to find more noise in these measurements. In particular, Piñeiro et al. (2021) have shown that the ribs present enormous variability. Ribs are possibly the only bone in *Mesosaurus* that does not follow any pattern. There is no correlation between the mean width of the ribs and the mean width of the femur.

Isometric growth is a rare phenomenon among reptiles, and in general among tetrapods. Only some salamanders and frogs are known to display it (Protero 2013). Based on the comparison of cranial features of Paleozoic taxa, Olori (2013) suggested that isometric growth is a plesiomorphic developmental pattern, an ancestral feature of development in early tetrapods, by which there is a strong correlation among bones during growth.

Ontogenetic series provide valuable information about life history, developmental, and evolutionary patterns in extinct taxa. These series are based in morphological investigations of fossil growth series. These series are rarely preserved in the fossil record, and when preserved are often incomplete and difficult to interpret. Among Palaeozoic and early Mesozoic tetrapods the best data come from aquatic and semi-aquatic species (Caldwell 1994, 1997, 2002; Piñeiro et al. 2016; Fröbisch et al. 2010; Atkins et al. 2020; among others). That is the case for the fossil record of *Mesosaurus*, where we find one of the most complete ontogenetic series (Piñeiro et al. 2016). In the present study we expand mesosaur ontogenetic series identifying six stages of ossification using the proximal tarsals (astragalus, calcaneum, and navicular). Fig. 13 summarizes the ossification degree and size of the different tarsal bones associated with ontogenetic stage. Moreover, we show that ontogenetic series correlate with size of the individuals, a fascinating feature of mesosaurs that is not seen in many

other basal amniotes. As first approximation, we can state, based on ontogenetic series, that stage *i* characterizes the foetal stage, stages ii and *iii* the juveniles, stage *iv* the young adults (or sub-adults) and stages *v* and *vi* the "elder" adults (see also Piñeiro et al. 2016).

Incipient ossification of the astragalus and calcaneum suggests a juvenile specimen far from maturity. Young adults are characterized by a quadrangular astragalus in contact with a roughly triangular calcaneum, shaping an incipient foramen for the perforating artery, as well as rounded centralia (i.e. not developed navicular). Adults are characterized by a well-formed astragalus and calcaneum with a well-defined foramen for the perforating artery; a well-developed navicular of transversely elongated shape. The "elder" stage will be achieved when the navicular completes its fusion with the astragalus.

Something similar can be suggested for the carpus, which is devoid of ossified bones in the initial stages of development until the intermedium and the ulnare appear, along with a large central bone formed by the fusion of at least two bones. The appearance of an ossified distal carpal series and the fusion of intermedium with the central large bone (laterale centrale) purportedly complete the process of full maturity.

Previous and recent studies also suggest a strong correlation between tarsal development and scapulo-coracoid fusion, which not always is correlated with size (Piñeiro et al. 2016; Piñeiro et al. 2021). The scapula and the coracoid are preserved isolated in young individuals, but they tend to suture and fuse with each other during ontogeny, forming a unitary structure in adults. However, there are cases where small scapulo-coracoids are completely fused, and other significantly larger ones show both bones only barely articulated (Piñeiro 2002; Piñeiro et al. 2021). This suggests a pattern of variable ossification, similar to that occurring with the distal carpals and tarsals.

Unfortunately, the best-preserved scapulo-coracoids are disarticulated and isolated, thus precluding confident evaluation of the ontogenetic stage in which the fusion of these bones was completed, so a correlation of its size and status in relation to other bones should be studied further in the future.

On other hand, it is worth noting that long bone histology and skeletochronology have been considered as the most important and reliable tool for determining the absolute ontogenetic age of fossil vertebrates (Scheyer et al. 2010). However, the available histological information for mesosaurs (Nopcsa and Heidsieck, 1934; de Ricqlès, 1974; Klein et al. 2019) presents several problems:

i) Until now Mesosauridae has been considered as including three different species. However, recent research by Piñeiro et al. (2021), have argued that only *Mesosaurus tenuidens* is a valid taxon and *Stereosternum tumidum* and *Brazilosaurus sanpauloensis* are junior synonyms of the former, a statement that is supported by the results of the present study. Therefore, microanatomical studies based on the presence of differences associated with taxonomic assignation of the analyzed bones are questionable. For example, the study performed by Klein et al. (2019), where the authors found histological differences in the analyzed bones coming from some articulated skeletons that they assumed to belong to *Stereosternum* and to *Brazilosaurus* by the presence of autapomorphies that are demonstrated to have no taxonomic relevance (e.g., Piñeiro, 2002, 2006, 2008; Laurin and Piñeiro, 2017; Piñeiro et al. 2021). Klein et al. (2019) analysed eleven specimens catalogued as *Brazilosaurus* and reclassified ten of them as *Stereosternum* based on the number of presacral vertebrae, neck/skull ratio and degree of pachyosteosclerosis of the ribs. However Piñeiro et al. (2021) have shown that these criteria are not valid to separate three monotypic mesosaur taxa. Furthermore, Piñeiro et al. (2021) show that neck length against skull length ratio

is constant and the same for all the purported species, i.e there is isometric growth between the neck and the skull, highly consistent with the results of the present study. Moreover, these authors did not describe the histology of *Mesosaurus tenuidens* but rather they rely on the work of de Ricqlès, (1974), who describe a hindlimb and "fragments" of ribs and long bones, which a priori cannot be assigned to any species due the lack of diagnostic characters.

ii) All the available studies concentrate on the pachyostosis or osteosclerosis of the specimens. None of the papers correlates or analyses the ontogenetic state of their specimens -except perhaps for one specimen studied by de Ricqlès (1974).

iv) According to Klein et al. (2019): "*double or even multiple rest lines at the end of each cycle, making exact growth mark counts difficult and pointing to a high influence of exogenous (e.g. several growth season per annum) and endogenous (e.g. several reproduction cycles per annum) factors*". Moreover, Piñeiro et al. (2021) have argued about the possibility that variations in salinity are responsible for the variations observed in the pachyosteosclerosis of mesosaur ribs (see also Chang et al. 2008). It is worth remembering that the Permian sea in which the mesosaurs lived dried up and evaporitic minerals were deposited mixed with events of high mortality (Piñeiro et al., 2012c). Despite these issues, according to our ontogenetic and developmental series, measurements for the humerus and femur reported by Klein et al. (2019) for their eleven studied specimens are consistent with the size expected for ontogenetic stages *iii*, *iv* and *v*. Thanks to images of some of the studied specimens kindly provided by the authors (A. Verrière, MfN Berlin, *personal communication*, 2021) we could corroborate the ontogenetic stage in four of these specimens preserving the tarsus. Although Klein et al. (2019) state that there is no correlation of size with number of growth marks (age), eight out of eleven studied specimens do correlate well number of growth marks with

humerus and femur lengths. In fact, removing only the two most extreme specimens, the correlation between size and reported age becomes 0.8 among the nine remaining specimens. According to their data, specimens in the stage *iii* would be between 1 or 2 years old, specimens in the stage *iv* would be between 2 to 4 years old, and specimens in the stages *v* between 4 and 5 years old. Moreover, de Ricqlès (1974) analysed a specimen with a perfectly ossified tarsus, with a fused navicular (stage *vi*) suggesting that it is between 6 and 7 years old (see de Ricqlès, 1974, figure 10).

The two most divergent specimens in Klein et al. (2019) belong purportedly to category iii, due to their size but were assigned at least 7 years old to them. However, without additional data, it is only possible to speculate on its implication. These are undoubtedly specimens that could be fundamental to validate both the ontogenetic series and the determination of an absolute age for mesosaurs from the study of histological sections. One possible explanation is that the endogenous and exogenous variations are so high that it is extremely difficult, if not impossible, to determine the age of mesosaurs through histological sections. Another possibility could be the existence of miniaturization among mesosaurs (Piñeiro et al. 2021), in that case, due to the strong isometry, these could not be differentiated from the rest but only by histological sections or the degree of pachyosteosclerosis. This could also account for previously discussed variations in ossification and for the differences previously attributed to the presence of more than one species of mesosaurs, currently synonymised to *Mesosaurus*.

4.2. Phalanx modularity and Evolution

Phalanges form by a process of sequential segmentation along the toe axis. Each toe grows from the so-called “digit-forming region” continuously adding cells to the distal end of the bone. When the cartilage reaches a critical length, a segmentation process occurs, creating a joint behind the growing tip. The process is repeated several times, giving rise to the different phalanges (Kavanagh et al. 2013). Theory suggests that toes are morphological modules, strongly interrelated, in which development strongly controls the phenotypic variations.

The phalangeal and tarsal proportions of *Mesosaurus* and *Hovasaurus* are relatively constant throughout life; and as was noted by Currie (1981), this implies that they must have grown at approximately the same rate. *Hovasaurus* has a strong modularity in each digit, but less linkage between them. The 2nd, 3th and 4th digits seem to have a modular behaviour sharing their proportions, while the first and fifth digits diverge from the pattern; their first phalanx is much greater than expected, with almost the same size as the metatarsal. The penultimate phalanx in each toe of *Hovasaurus* is almost the same size (even slightly higher) than the previous phalanx, and this is seen as an almost constant pattern in the graphics (Figs. 16, 18, 20).

Such a feature is not noted in mesosaurs, in which, conversely, the lack of independence among metatarsals and phalanges suggests that there might be a strong developmental linkage between the formation of successive phalanges in a growing digit, where there is a dramatic decrease in size from phalanx to phalanx (Eble et al. 2005; Kavanagh et al. 2013; Young et al. 2015). This pattern involves a low degree of differentiation/parcellation of existing elements, probably associated with an ancestral evolutionary pattern (Piñeiro et al. 2016).

4.3 5th toe – the longest toe

It is quite unusual to find species with five or more digits that present the digital sequence ordered by size as seen in mesosaurs, with the fifth being the longest, (Holder 1983). In general, animals that have total or partial loss of the digit V do present such character, but with the IV finger being the longest (see Holder 1983).

There are few references of animals possessing five digits with this character. Sea otters present a similar pattern in their hindlimbs (Adam 2009) and pinnipeds (Otariidae and Phocidae) in the forelimbs (Koretsky et al. 2016). Interestingly, phocids and sea otters swim by lateral undulation and use their fins/limbs as stabilizers, although they can alternate undulation with paddling (Tarasoff et al. 1972; Fish 1994). The same swimming pattern was suggested for mesosaurs, although mainly for their hindlimbs (Villamil et al. 2015). Moreover, pinnipeds are also semi-aquatic, a characteristic that was also suggested for mesosaurs (Nuñez Demarco et al. 2018). Conceivably, this structural pattern derives from a convergent evolution by development of similar adaptive traits to semi-aquatic environments, but the differences between the compared groups are so great that it may be simply the result of stochastic evolution (Stayton 2015).

4.4. Implications of the isometric growth pattern found in mesosaurs regarding their controversial phylogenetic relationships

4.4.1. The suggested mesosaur-parareptilian relationship

The phylogenetic relationships of mesosaurs are not yet resolved because they were found to be basal sauropsids (Laurin and Reisz, 1995; Laurin and Piñeiro, 2017, 2018) but other research placed them as basal parareptiles (e.g. Modesto, 1999; MacDougall et

al., 2018, Ford and Benson, 2020). Indeed, in a recent phylogenetic study, Laurin and Piñeiro (2017) found that mesosaurs can occur in different positions, but always outside the smallest clade that includes all the other sauropsids, and in many trees they are the sister group of Amniota. Many characters support the basal phylogenetic position of mesosaurs, mainly because they are morphologically highly conservative (Piñeiro et al. 2012b; 2021).

Mesosaurs and parareptiles have several differences; at the level of the skull, mesosaurs possesses a synapsid-like small lower temporal fenestra, while most parareptiles are anapsids (see discussion in Piñeiro et al. 2012b and Laurin and Piñeiro 2017, 2018 for additional information), coincident to which can be expected in cotylosaurs (Romer, 1956). Some specializations that have been considered as derived in mesosaurs, such as the long snout, the delicate and long teeth, and the pachyosteosclerosis of their skeleton (Canoville and Laurin 2010), are mainly adaptations to a semiaquatic lifestyle (Núñez Demarco et al., 2018). Conversely, parareptiles are mostly terrestrial. Even though mesosaurs share some features with parareptiles, such as the swollen morphology of the neural arches of dorsal vertebrae, a feature that is also present in other groups of basal amniotes as capthorinids and protorothyrids (e.g., Müller et al., 2006), some basal synapsids (e.g., Sumida, 1989), and also in "microsaurian" lepospondyls (Vaughn, 1962). Thus, we could assume that this is a plesiomorphic condition that has developed independently in these groups.

Regarding the phylogenetic hypotheses that suggested a mesosaur-parareptile relationship, we can see that after Gauthier et al. (1988), mesosaurs are basal to a clade formed by Procolophonia + Pareisauridae + Milleretidae. Other more recent papers including mesosaurs (e.g., Müller and Tsuji, 2007), also show them in a basal position (almost like an outgroup), with respect to all other parareptilians, and when mesosaurs

are considered as a clade formed by the three previously proposed taxa (*Mesosaurus*, *Stereosternum* and *Brazilosaurus*) (see Tsuji and Müller, 2009, figure 3, page 78), they recovered unresolved relationships, as would be expected when comparing specimens belonging to the same taxon (Piñeiro et al., 2021). On the other hand, mesosaurs were not considered in the phylogenies of Lee (1997) and Rieppel and Reisz (1999) in their study of parareptilian relationships. More recently, studies performed by MacDougall et al. (2018) and Ford and Benson (2020) on early amniote relationships found mesosaurs nested within Parareptilia again at the basalmost position of this clade. The MacDougall et al., (2018) paper includes a critical view to a previously published phylogeny by Laurin and Piñeiro (2017) which reassessed the position of mesosaurs as the sister taxon of all other sauropsids. They found two main problems that may have produced that topology: i) basing the analysis on an "outdated" matrix and therefore "ignoring" the hypotheses that have placed mesosaurs as basal parareptiles (obviously, the one that they support) and ii) considering mesosaurs as having a synapsid-like temporal fenestra, which after MacDougall et al. (2018) is a character variable among the mesosaur species. Laurin and Piñeiro (2018) downplayed the concerns of Mac Dougall et al. (2018), mainly because not only the Laurin and Reisz (1995) matrix had been completely outdated but also because even considering mesosaurs as having a synapsid-like temporal fenestra, the mesosaur relationships were vindicated by the new analysis. Furthermore, the results from Laurin and Piñeiro (2017) were not as surprising as those from MacDougall et al. (2018), where parareptiles were nested within Diapsida and the "Pelycosauria" were recovered as paraphyletic.

Two years later, another study by Ford and Benson (2020) vindicated the topology of MacDougall et al. (2018) in which mesosaurs are nested within Parareptilia, but split them into *Mesosaurus* and *Stereosternum* with no explanation for the exclusion

of *Brazilosaurus*. This mesosaur topology recovered by Ford and Benson (2020), is improbable in light of the idea that *Stereosternum* has been recently demonstrated to be the junior synonymous of *Mesosaurus* (Piñeiro et al., 2021). Moreover, this last paper also showed parareptiles nested within Diapsida, a result previously found by Piñeiro (2004; 2008), by Laurin and Piñeiro (2017), and by MacDougall et al. (2018). Therefore, it is worth highlighting that it is a reluctant result obtained from differently coded and analyzed matrices. As in MacDougall et al. (2018), Ford and Benson (2020) also show a paraphyletic Synapsida, where varanopids are also nested within Diapsida. However, a revision of the character distribution in the taxa that support the new topology for the Varanopidae outside Synapsida, which historically, and until just few years ago, had been considered as the most diverse and long-lived group of basal synapsids (Reisz & Dilkes, 2003), is worthwhile, mainly to verify that the results from MacDougall et al. (2018) and Ford and Benson (2020) were not influenced by misidentifications of diapsids as synapsids and vice versa, as has occurred more than once in the past (e.g., Reisz et al., 2010).

4.4.2. Mesosaurs as early amniotes

As previously mentioned, the traditional study of Laurin and Reisz (1995) recovered mesosaurs to be basal sauropsids, which are the sister taxon of the Parareptilia+Eureptilia clade.

If this hypothesis is correct mesosaurs should share some more features with taxa that have been considered as the earliest reptiles such as *Hylonomus lyelli* (Carroll, 1964) and particularly *Westlothiana lizziae* a taxon that was described as the oldest known reptile (Smithson, 1987) and later degraded to a stem amniote tetrapod of

uncertain relationship (Smithson et al., 1994, but see also Piñeiro et al. 2016). Considering that Mesosauridae seems to be represented by only *Mesosaurus tenuidens* (Piñeiro et al., 2021) a possible phylogenetic frame may be to consider them as an early diverging basal sauropsid branch, being sterile in that they were not ancestral to any other later amniote group. However, this hypothesis would yet need to be corroborated. One way to do so is by calibrating *Mesosaurus* with respect to the earliest amniotes, i.e. *Hylonomus lyelli* and their roughly contemporaneous *Paleothyris acadiana*, and also to *Westothiana lizzie*, which although controversial, has been considered as a stem amniote in most analyses, and even very close to "microsaurs" (Marjanović and Laurin, 2013; Didier et al. 2019). Only a few phylogenetic studies on early amniotes have included *Hylonomus* as an OTU, possibly because the holotype of this taxon is a completely disarticulated specimen that does not allow the morphology of the temporal region of the skull to be clearly determined, although it was suggested that it resembled other basal eureptiles (Carroll, 1964). Therefore, the *Hylonomus* skull restoration was not exclusively based on the holotype specimen (BM(NH) R.4168) but on other different materials found at the same locality, that consist also of disarticulated bones. Even still, a recent phylogeny (i.e., Ford and Benson 2020) recovered *Hylonomus* as the basalmost taxon of a clade including *Anthracodromeus*, *Paleothyris* and *Protorothyris*, which is the sister group of Captorhinidae at the base of Reptilia; it is not recovered as the basalmost amniote. Perhaps a reappraisal of the comparative anatomy and relationships of all the specimens assigned to *Hylonomus lyielli*, including the holotype and the purported conspecifics and contemporaneous taxa from the Joggins Formation (Mann et al., 2020) would be necessary in order to update the identity of those materials upon which the oldest known reptile was restored.

Considering that mesosaurs have a conservative skeletal morphology, as can be expected for a basal amniote, and proving that isometry is the main mesosaur growth pattern as we have done herein, is outstanding and may introduce new hypotheses about their relationships that have not been considered before. Moreover, mesosaur hindlimb proportions are thought to be remarkably similar to those of stem-amniote (i.e., *Gephyrostegus*), amniotes (i.e. *Captorhinus*) but also stem-tetrapods (i.e. *Tulerpeton curtum*) (see Nuñez Demarco et al. 2018, fig. 12) while the structure of its tarsus is very similar to that of Reptilia (i.e. *Hylonomus*, *Captorhinus*, *Petrolacosaurus*) or even "microsaurs" (i.e. *Tuditanus*, *Pantylus*) (see Piñeiro et al. 2016, fig. 10).

Unfortunately, it is not possible to evaluate the presence of similar growth patterns in *Hylonomus* and their relatives (Ford and Benson, 2020) nor in other basal eureptiles, because the available number of individuals within each taxon is generally very low and it is not possible to test the rate of allometric changes that can occur during ontogenetic development, at least not with the precision that is observed in mesosaurs. Furthermore, we cannot affirm that the isometric growth is an aberrant or derived strategy exclusive for mesosaurs. On the contrary, we do know that isometry was the primary general growth pattern for some microsaurs, based on geometric morphometric analyses performed in large samples of *Microbrachis pelikani and Hyloplesion longicostatum* (100 and 18 specimens analysed, respectively). The obtained results have determined that the growth patterns in these taxa would be the ancestral condition for at least stem amniotes if not for Tetrapoda (Olori, 2013, 2015).

The Lepospondyli (Zittel, 1888) are a highly diverse group (Orders: Microsauria, Adelospondyli, Aistopoda, Nectridea, Lysorophia) of small-to-mid sized tetrapods spanning from Early Carboniferous to Early Permian in age. Lepospondyli have been proposed both to be related to the origins of Lissamphibia (the 'lepospondyl

hypothesis', e.g., Marjanović and Laurin, 2009, 2013, 2018) or considered close of the origin of Reptilia or Amniota (i.e. Vaughn, 1962; Carroll, 1995; Anderson, 2007; Pardo et al., 2017). Furthermore, recent phylogenetic and anatomical studies (Anderson, 2007; Pardo et al., 2017, Pardo and Mann, 2018; Mann and Maddin, 2019; Mann et al. 2019; Mann et al. 2020; Mann et al., 2021) have further supported the polyphyly of Lepospondyli (e.g. aistopods as stem-tetrapods) and recovered a central core-grouping of 'microsaurs' called the Recumbirostra (Anderson, 2007; Huttenlocker et al., 2013) as crown-group amniotes. This recent result from Pardo et al. (2017) also recovers lysorophians within Recumbirostra (*further supported by* Mann et al., 2019), together both are recovered as early reptiles, while other lepospondyl clades remain as either stem amniotes (e.g. Nectridea) or stem-tetrapods (e.g. Aistopoda). Intriguingly, according to these authors, the new results should not affect the position of other taxa, particularly such of *Westlothiana* in the Amniota stem, even if this taxon is not included in the performed analysis.

4.4.3. *Mesosaurus tenuidens* and the evolutionary paths for the isometric growth pattern

These previous studies and the results presented herein for *Mesosaurus tenuidens* allow us to strengthen previous hypotheses of stem and early amniote evolution (Olori, 2013, 2015) and reassess isometry as the main growth pattern characterizing the earliest reptiles. According to what is known about growth patterns for later groups, allometry appears to be most common and widespread. To investigate this last hypothesis in extinct more derived sauropsid groups, we compared our results for *Mesosaurus* with the diapsid *Hovasaurus boulei*, a Permian reptile from Madagascar that is thought to

have had a similar lifestyle and for which an enough large sample is available (see above). We found that *Hovasaurus*´s growth pattern is not comparable with that seen in mesosaurs. Among other later fossil reptiles, there may be some kind of isometric growth in psittacosaur ceratopsian dinosaurs, meaning that the skull grows according to the age of the individual (Zhao et al., 2014). However, references for the postcranial skeleton are scarce and they suggest more or less marked allometry.

The evolutionary path for isometric growth in basal amniotes is shown in Figure 21, taking into account the last and more widespread phylogenetic hypotheses. There, we can see that the most parsimonious hypothesis may be that shown in Fig. 21A: i.e. mesosaurs in a close relationship to some 'lepospondyl' groups, unless isometry is considered as an evolutionary condition that was independently acquired by these taxa (Fig. 21 B). In support of the first possibility, mesosaurs and some 'lepospondyl' groups do not share only the isometric growth pattern, but also a particular combination of characters that would ally them, such as their elongated bodies, their tendency to lighten the skull by developing openings, the tendency to increase the number of presacral and caudal vertebrae, the possession of strongly amphicoelus vertebrae, swollen neural arches and the absence of suture lines between centrum and neural arches, as is common for the groups that form the stem Amniota (see Danto et al., 2016). The evolutionary significance of these combined shared characters should be analyzed in a phylogenetic context and perhaps new hypotheses of relationships may arise for mesosaurs.

4.5. Methodological fitness

As can be seen, the employed methodology is not one hundred percent accurate, because environmental and ecological factors could constrain the degree of ossification

of the bones and the growth rate. Nevertheless, it has enormous potential, particularly for the classification or identification of disarticulated material. Therefore, our results can be useful for the identification of different individuals represented in bone beds as well as their ontogenetic stages. It also allows for recognition of size groups in the complex preservation of several juxtaposed individuals, increasing our understanding of biological behaviours of the species.

Furthermore, the morphometric studies performed herein permit us to support the hypothesis that mesosaurs are represented by only one species. Perhaps diagnostic characters were more evident at the level of soft tissues or different biological behaviours, but this is difficult to ascertain from fossils. Our study also supports recent studies that suggest that the variation observed in mesosaurs is due to ontogeny, intraspecific variability derived from environmental factors, and/or from taphonomy, and possibly sexual dimorphism (Piñeiro et al. 2021). In this sense, it is worth noting that isometry is commonly associated with low morphological diversity (McNamara 1997; Sears et al. 2007; Sanchez-Villagra 2010).

5. Conclusions

The morphometric study performed herein represents the first ontogenetic reconstruction of the cranial and postcranial ossification sequence in mesosaurs. More than one hundred specimens examined, including the skull, vertebral column and limbs of *Mesosaurus tenuidens*, have demonstrated isometric growth for mesosaurs during their development, meaning that there is a notable relationship between age and size. Isometric growth implies that all body parts increase in size at the same rate and the

juvenile proportions are not different from those of the adults. This is a rare phenomenon among reptiles, and also among tetrapods.

Comparative morphometric analyses performed on a more derived sauropsid such as *Hovasaurus boulei* suggest that while this taxon is adapted to semiaquatic environments like mesosaurs, it stopped growing at a determinate size, so is represented by small juvenile and larger adult individuals. In contrast, mesosaurs display a continuous and gradual growth pattern with individuals representing all the ontogenetic stages.

The anatomical structure of the carpus was also reappraised and a review of the available literature revealed substantial subjectivity among the authors that described it. The present study shows that the identity of the constituent carpal bones (as consistently with the tarsals) depends on the degree of ossification and fusion of the elements throughout ontogeny. Therefore, the differences previously proposed to separate mesosaur taxa on the basis of carpus (and tarsus) structure cannot be supported.

The phalangeal and tarsal proportions of *Mesosaurus* and *Hovasaurus* are relatively constant throughout life, and both have strong modularity in each digit. However, in mesosaurs there might be a strong developmental linkage between the formation of successive phalanges in a growing digit, with a dramatic decrease in size from phalanx to phalanx. Moreover, the strong modularity among metatarsals and phalanges seen in mesosaurs is also very unusual and suggests a very primitive pattern.

Furthermore, the morphometric data obtained in this study strongly support the hypothesis that there is no more than one mesosaur taxon, and the variations observed reflect the influence of environmental conditions, taphonomical features and intraspecific variation (Piñeiro et al. 2021).

Detection of isometric growth in mesosaurs is consistent with previous observations that suggested the presence of plesiomorphic features in their anatomy

(Huene 1940, 1941; Piñeiro et al. 2016; Nuñez Demarco et al. 2018). Many of these features along with the isometric pattern of growth are shared with those present in "microsaurian" tetrapods which were recovered as basal amniotes in recent phylogenies (Pardo et al. 2017; Mann et al. 2019; Gee et al. 2020). The results obtained herein would be relevant to reassess mesosaur phylogenetic relationships and to support recent radiometric and biostratigraphic studies in the mesosaur-bearing Mangrullo Formation of Uruguay, which suggest that mesosaurs may be older amniotes than previously thought (Calisto and Piñeiro 2019).

In light of the new results, we are willing to suggest that mesosaurs were not the oldest group of reptiles that returned to the aquatic environment and that their ancestors may have been animals that were adapted to live within or close to water bodies.

Acknowledgments

We specially thank Pablo Velozo for have taken the photographs of the *Hovasaurus* specimens housed at the MNHN of Paris and Melitta Meneghel for valuable comments and suggestions on the original manuscript. We are very indebted to James O. Farlow and to Arjan Mann for their useful comments and suggestions that very much improved the first version of this manuscript. Facultad de Ciencias, National Geographic and ANII grants to GP and JF, financed the different steps of research that derived in the present study.

References

Anderson, J. S. 2007. Incorporating ontogeny into the matrix: a phylogenetic evaluation of developmental evidence for the origins of modern amphibians; pp. 182–227

in J.S. Anderson and H.-D. Sues (eds.) Major Transitions in Vertebrate Evolution. Indiana University Press, Bloomington.

Anderson, T.L., Ousterhout, B.H., Drake, D.L., Burkhart, J.J., Rowland, F.E., Peterman, W.E. and Semlitsch, R.D. 2016. Differences in larval allometry among three ambystomatid salamanders. Journal of Herpetology 50(3): 464-470.

Araújo, D. C. 1977. Taxonomia e relações dos Proganosauria da Bacia do Paraná. Anais da Academia Brasileira de Ciências 48: 91–116.

Berman, D. 2000. Origin and early evolution of the amniote occiput. Journal of Paleontology 74(5): 938–956.

Bickelmann, C. and Tsuji, L.A. 2018. A case study of developmental palaeontology in *Stereosternum tumidum* (Mesosauridae, Parareptilia). Fossil Record 21: 109–118. https://doi.org/10.5194/fr-21-109-2018

Bonnan, M.F. 2004. Morphometric analysis of humerus and femur shape in Morrison sauropods: implications for functional morphology and paleobiology. Paleobiology 30(3): 444–470.

Bonnan, M.F. 2007. Linear and geometric morphometric analysis of long bone scaling patterns in Jurassic neosauropod dinosaurs: their functional and paleobiological implications. The Anatomical Record: Advances in Integrative Anatomy and Evolutionary Biology: Advances in Integrative Anatomy and Evolutionary Biology 290(9):1089–1111.

Bonnan, M.F., Farlow, J.O. and Masters, S.L. 2008. Using linear and geometric morphometrics to detect intraspecific variability and sexual dimorphism in femoral shape in *Alligator mississippiensis* and its implications for sexing fossil

archosaurs, Journal of Vertebrate Paleontology 28(2): 422–431. http://dx.doi.org/10.1671/0272-4634(2008)28[422:ULAGMT]2.0.CO;2

Caldwell, M.W. 1994. Developmental constraints and limb evolution in Permian and modern lepidosauromorph diapsids. Journal of Vertebrate Paleontology 14: 459–471.

Caldwell, M.W. 1997. Limb ossification patterns of the ichthyosaur *Stenopterygius*, and a discussion of the proximal tarsal row of ichthyosaurs and other neodiapsid reptiles. Zoological Journal of the Linnean Society 120(1):1–25.

Caldwell, M.W. 2002. From fins to limbs to fins: limb evolution in fossil marine reptiles. American Journal of Medical Genetics 112(3): 236–249.

Calisto, V. and Piñeiro, G. 2019. A large cockroach from the mesosaur-bearing Konservat-Lagerstätte (Mangrullo Formation), Late Paleozoic of Uruguay. PeerJ, 7, e6289.

Carroll, R. 1981. Plesiosaur ancestors from the Upper Permian of Madagascar. Philosophical Transactions of the Royal Society B 293:315–383.

Carroll, R.L. 1982. Early evolution of reptiles. Annual Review of Ecology and Systematics 13: 87–109.

Carroll, R.L. 1995. Problems of the phylogenetic analysis of Paleozoic choanates. Bulletin du Muséum National d'Histoire Naturelle, Section C. Series 4. 17 (1–4): 389–445.

Canoville, A. and Laurin, M. 2010. Evolution of humeral microanatomy and lifestyle in amniotes, and some comments on paleobiological inferences. Biological Journal of the Linnean Society 100: 384–406. doi: 10.1111/j.1095-8312.2010.01431.x

Chang, M.; Wang, X.; Liu, H.; Miao, D.; Zhao, Q.; Wu, G.; Liu, J.; Li, Q.; Sun, Z. & Wang, N. 2008. Extraordinarily thick-boned fish linked to the aridification of the Qaidam Basin (northern Tibetan Plateau). Proceedings of the National Academy of Sciences, 105:13246–13251. doi:10.1073/pnas.0805982105

Cope, E.D. 1885a. A contribution to the vertebrate paleontology of Brazil. Paleontological Bulletin 40:1–21. Philadelphia.

Currie. 1981. *Hovasaurus boulei*, an aquatic eosuchian from the upper Permian of Madagascar. Palaeontographica Africana 24:99–168.

Danto, M., Witzmann, F. and Frobisch, N. 2016. Vertebral development in Paleozoic and Mesozoic tetrapods revealed by paleohistological data. PLoS One 11(4): e0152586. doi: 10.1371/journal.pone.0152586

Didier, G. Chabrol, O. and Laurin, M. 2019. Parsimony-based test for identifying changes in evolutionary trends for quantitative characters: implications for the origin of the amniotic egg. Cladistics, Wiley 35 (5) 576-599. Doi: 10.1111/cla.12371.hal-01609238

Eble, G.J., Callebaut, W. and Rasskin-Gutman, D. 2005. Morphological modularity and macroevolution: conceptual and empirical aspects. Modularity: understanding the development and evolution of natural complex systems 221–239 pp.

Fabrezi, M., Abdala, V. and Martínez Oliver, M.I. 2007. Developmental basis of limb homology in lizards. The anatomical record 290: 900–912.

Farlow, J. O. (2018). Noah's ravens: Interpreting the makers of tridactyl dinosaur footprints. Indiana University Press.Feng, C., Wang, H., Lu, N., Chen, T., He, H., Lu, Y., and Tu, X.M. 2014. Log-transformation and its implications for data analysis. Shanghai archives of psychiatry 26(2): 105–109. https://doi.org/10.3969/j.issn.1002-0829.2014.02.009

Fish, F.E. 1994. Association of propulsive swimming mode with behaviour in river otters (*Lutra canadensis*). Journal of Mammalogy 75(4): 989–997.

Ford, D.P. and Benson, R.B.J. 2020. The phylogeny of early amniotes and the affinities of Parareptilia and Varanopidae. Ecology and Evolution 4(1): 57–65. DOI: 10.1038/s41559-019-1047–3

Gee, B.M. Bevitt, J.J. and Reisz, R.R. 2021. Computed tomographic analysis of the cranium of the early Permian recumbirostran 'microsaur' *Euryodus dalyae* reveals new details of the braincase and mandible. *Papers in Palaeontology*, *7*(2): 721–749.

Gervais, P. 1865. Description du *Mesosaurus tenuidens*, reptile fossile de l'Afrique australe. Académie des Sciences et Lettres de Montpellier Mémoires de la Section des Sciences, Tome Sixième. Boehm et Fils, Montpellier, 169–175.

Holder, N. 1983. Developmental constraints and the evolution of vertebrate digit patterns. Journal of theoretical biology 104(3): 451–471.

Huene F. von. 1940. A idade Permiana inferior de todas as camadas contendo mesossáurios. Divisão de Mineração e Metalurgia 6: 64–68.

Huene F. von. 1941. Osteologie und systematische Stellung von *Mesosaurus*. Palaeontographica, Abteilung A 92:45–58.

Huttenlocker, A.K., Pardo, J.D. Small, B.J. and Anderson, J. 2013. Cranial Morphology of Recumbirostrans (Lepospondyli) from the Permian of Kansas and Nebraska, and Early Morphological Evolution Inferred by Micro-Computed Tomography. Journal of Vertebrate Paleontology 33(3): 540–552. DOI: 10.1080/02724634.2013.728998

Huxley, J.S. 1924. Constant differential growth rates and their significance. Nature 144:895–896.

Jolicoeur, P. and Mosimann, J.E. 1968, Intervalles de confiance pour la pente de l'axe majeur d'une distribution normale bidimensionnelle. Biométrie-Praximétrie 9:121–140.

Kavanagh, K.D., Shoval, O., Winslow, B.B., Alon, U., Leary, B.P., Kan, A. and Tabin, C.J. 2013. Developmental bias in the evolution of phalanges. Proceedings of the National Academy of Sciences 110(45): 18190–18195.

Koretsky, I.A., Barnes, L.G. and Rahmat, S.J. 2016. Re-evaluation of morphological characters questions current views of pinniped origins. Vestnik zoologii 50(4): 327–354.

Kowalewski, M. and Novack-Gottshall, P.M. 2010. Resampling methods in paleontology. Quantitative methods in paleobiology. Short Courses in Paleontology 16: 19–54.

Kuhn, O. 1969. Handbuch der Paläoherpetologie, Teil 9 Stuttgart: Gustav Fischer Verlag. 73 pp.

Laurin, M. and Reisz, R.R. 1995. A reevaluation of early amniote phylogeny. Zoological Journal of the Linnean Society 113:165–223. doi: 10.1111/j.1096-3642.1995.tb00932.x

Laurin, M. and de Buffrénil, V. 2016. Microstructural features of the femur in early ophiacodontids: a reappraisal of ancestral habitat use and lifestyle of amniotes. Comptes Rendus Palevol 15: 115–127. doi: 10.1016/j.crpv.2015.01.001

Laurin, M. and Piñeiro, G.H. 2017. A reassessment of the taxonomic position of mesosaurs, and a surprising phylogeny of early amniotes. Frontiers in Earth Science 5: 88.

Laurin, M. and Piñeiro, G.H. 2018. Response: Commentary: A reassessment of the taxonomic position of mesosaurs, and a surprising phylogeny of early amniotes. Frontiers in Earth Science 6: 220.

Leduc, D.J. 1987. A comparative analysis of the reduced major axis technique of fitting lines to bivariate data. Canadian Journal of Forest Research 17(7): 654–659.

Lee, M. S.Y. 1997. Pareiasaur phylogeny and the origin of turtles. Zoological Journal of the Linnean Society 120: 197–280.

Liu, J. and Bever, G.S. 2015. The last diadectomorph sheds light on Late Palaeozoic tetrapod biogeography. Biological Letters, 11: 20150100. http://dx.doi.org/10.1098/rsbl.2015.0100

Mann, A., Gee, B.M., Pardo, J.D., Marjanović, D., Adams, G.R., Calthorpe, A.S. and Anderson, J.S. 2020. Reassessment of historic ‘microsaurs’ from Joggins, Nova Scotia, reveals hidden diversity in the earliest amniote ecosystem. *Papers in Palaeontology*, *6*(4): 605–625.

Mann, A., and *Diabloroter bolti*, a short-bodied recumbirostran 'microsaur'from the Francis Creek Shale, Mazon Creek, Illinois. *Zoological Journal of the Linnean Society*, *187*(2): 494–505.

Mann, A., Pardo, J.D. and Maddin, H.C. 2019. *Infernovenator steenae*, a new serpentine recumbirostran from the 'Mazon Creek'Lagerstätte further clarifies lysorophian origins. *Zoological Journal of the Linnean Society*, *187*(2), 506–517.

Mann, A., Calthorpe, A.S. and Maddin, H.C. 2021. *Joermungandr bolti*, an exceptionally preserved 'microsaur'from the Mazon Creek Lagerstätte reveals patterns of integumentary evolution in Recumbirostra. *Royal Society Open Science*, *8*(7): 210319.

MacDougall, M.J., Modesto, S.P., Brocklehurst, N., Verrière, A., Reisz, R.R. and Fröbisch, J. 2018. Commentary: a reassessment of the taxonomic position of mesosaurs, and a surprising phylogeny of early amniotes. Frontiers in Earth Science 6: 99.

Mac Gregor, J.H. 1908. "On *Mesosaurus brasiliensis* nov. sp. from the Permian of Brasil," In: White, I.C. (ed.). Commissão dos Estudos das Minas de Carvão de Pedra do Brasil, Parte II (Rio de Janeiro: National Press), 301–336.

McArdle, B. 1988, The structural relationship: regression in biology. Canadian Journal of Zoology 66: 2329–2339.

McNamara, K. 1997. Shapes of time: the evolution of growth and development. Johns Hopkins University Press. First Edition. 360 pp.

Marjanović, D. and Laurin, M. 2009. The origin(s) of modern amphibians: a commentary. Evolutionary Biology 36 (3): 336–338. doi:10.1007/s11692-009-9065-8. S2CID 12023942.

Marjanović, D. and Laurin, M. 2013. The origin(s) of extant amphibians: a review with emphasis on the "lepospondyl hypothesis. Geodiversitas 35: 207–272. doi:10.5252/g2013n1a8. S2CID 67823991.

Marjanović, D. and Laurin, M. 2019. Phylogeny of Paleozoic limbed vertebrates reassessed through revision and expansion of the largest published relevant data matrix. PeerJ 6:e5565 https://doi.org/10.7717/peerj.5565

Mitteroecker, P. and Bookstein, F. 2007. The conceptual and statistical relationship between modularity and morphological integration. Systematic biology 56(5): 818–836.

Modesto, S.P. 1996. The anatomy, relationships, and palaeoecology of *Mesosaurus tenuidens* and *Stereosternum tumidum* (Amniota: Mesosauridae) from the Lower Permian of Gondwana. Unpublished PhD. Thesis, University of Toronto, Toronto, Canada.1-280 p.

Modesto, S.P. 2006. The cranial skeleton of the Early Permian aquatic reptile *Mesosaurus tenuidens*: implications for relationships and palaeobiology. Zoological Journal of the Linnean Society 146: 345–368. doi: 10.1111/j.1096-3642.(2006)0.00205.x

Modesto, S.P. 2010. The postcranial skeleton of the aquatic parareptile *Mesosaurus tenuidens* from the Gondwanan Permian. Journal of Vertebrate Paleontology 30: 1378–1395. doi: 10.1080/02724634.2010.501443

Modesto, S.P., Scott, D.M., MacDougall, M.J., Sues, H-D., Evans, D.C., and Reisz, R.R. 2015. The oldest parareptile and the early diversification of reptiles. Proccedings of the Royal Society B 282: 20141912. doi: 10.1098/rspb.2014.1912

Müller, J., Berman, D.S., Henrici, A.C., Martens, T. and Sumida, S.S. 2006. The Basal Reptile *Thuringothyris mahlendorffae* (Amniota: Eureptilia) from the Lower Permian of Germany. Journal of Paleontology. 80 (4): 726–739.

Müller, J. and Tsuji, L. A. 2007. Impedance-matching hearing in Paleo-zoic reptiles: evidence of advanced sensory perception at an earlystage of amniote evolution.– PloS ONE, 2 (9): e889.doi:10.1371/journal.pone.0000889

Nuñez Demarco, P., Meneghel, M., Laurin, M., and Piñeiro, G. 2018. Was *Mesosaurus* a fully aquatic reptile? Frontiers in Ecology and Evolution 6: 109.

Oelofsen, B.W. 1981. An anatomical and systematic study of the Family Mesosauridae (Reptilia, Proganosauria) with special reference to its associated fauna and palaeoecological environment in the Whitehill Sea. Unpublished PhD. thesis, University of Stellenbosch, South Africa. 250 pp.

Oelofsen, B. and Araújo, D.C. 1987. *Mesosaurus tenuidens* and *Stereosternum tumidum* from the Permian Gondwana of both southern Africa and South America. South African Journal of Science 83:370–372.

Olori, J.C. 2013. Morphometric analysis of skeletal growth in the lepospondyls *Microbrachis pelikani* and *Hyloplesion longicostatum* (Tetrapoda, Lepospondyli). Journal of Vertebrate Paleontology 33(6): 1300–1320.

Olori, J. 2015. Skeletal Morphogenesis of Microbrachis and Hyloplesion (Tetrapoda: Lepospondyli), and Implications for the Developmental Patterns of Extinct, Early Tetrapods. PLoS One 2015; 10(6): e0128333. doi: doi: 10.1371/journal.pone.0128333

Pardo, J.D., Szostakiwskyj, M., Ahlberg, P.E. and Anderson, J.S. 2017. Hidden morphological diversity among early tetrapods. Nature Letters. 546: 1–12. doi:10.1038/nature22966

Pardo, J.D. and Mann, A. 2018. A basal aïstopod from the earliest Pennsylvanian of Canada, and the antiquity of the first limbless tetrapod lineage. *Royal Society open science*, *5*(12):181056.

Piñeiro, G. 2002. Paleofaunas del Pérmico-Eotriásico de Uruguay. Unpublished MSc. Thesis. PEDECIBA, Universidad de la República, Montevideo, Uruguay, 208 pp.

Piñeiro, G. 2004. Paleofaunas del Pérmico y Permo-Triásico de Uruguay: Bioestratigrafía, Paleobiogeografía y Sistemática. Unpublished PhD. Thesis. PEDECIBA, Universidad de la República. Montevideo, Uruguay. 206 pp.

Piñeiro, G. 2006. Nuevos aportes a la paleontología del Pérmico de Uruguay. In: Veroslavsky, G. Martínez, S. and Ubilla, M. (eds.). Cuencas Sedimentarias de Uruguay– Paleozoico. DIRAC, Facultad de Ciencias. Montevideo, Uruguay, p. 257–279.

Piñeiro, G. 2008. Los mesosaurios y otros fósiles de fines del Paleozoico. In: Perea D. (ed). Fósiles de Uruguay. DIRAC. Facultad de Ciencias, Montevideo, Uruguay p. 179–205.

Piñeiro, G., Ferigolo, J., Meneghel, M. and Laurin, M. 2012a. The oldest known amniotic embryos suggest viviparity in mesosaurs. Historical Biology 24: 630–640. doi: 10.1080/08912963.2012.662230

Piñeiro, G., Ferigolo, J., Ramos, A. and Laurin, M. 2012b. Cranial morphology of the Early Permian mesosaurid *Mesosaurus tenuidens* and the evolution of the lower temporal fenestration reassessed. Comptes Rendus Palevol 11: 379–391. doi: 10.1016/j.crpv.2012.02.001

Piñeiro, G., Ramos, A., Goso, C., Scarabino, F., and Laurin, M. 2012c. Unusual environmental conditions preserve a Permian mesosaur-bearing Konservat-Lagerstätte from Uruguay. Acta Palaeontologica Polonica 57: 299–318. doi: 10.4202/app.2010.0113

Piñeiro, G., Ferigolo, J., Ribeiro, A.M. and Velozo, P. 2015. Reassessing the affinities of vertebral remains from Permo-Triassic beds of Gondwana. Comptes Rendus Palevol, 14: 387–401.

Piñeiro, G., Nuñez Demarco, P. and Meneghel, M.D. 2016. The ontogenetic transformation of the mesosaurid tarsus: a contribution to the origin of the primitive amniotic astragalus. PeerJ 4: e2036.

Piñeiro, G., Ferigolo, J., Mones, A. and Núñez Demarco, P. 2021. Mesosaur taxonomy reappraisal: are *Stereosternum* and *Brazilosaurus* valid taxa? Revista Brasileira de Paleontologia. 24(3): 205–235. doi:10.4072/rbp.2021.3.04

Protero, D.R. 2013. Bringing fossils to life. An introduction to Paleobiology. Columbia University Press. New York. Tirth Edition.672 pp.

Reisz, R.R. and Dilkes, D.W. 2003. *Archaeovenator hamiltonensis*, a new varanopid (Synapsida: Eupelycosauria) from the Upper Carboniferous of Kansas. Canadian Journal of Earth Science. 40: 667–678 (2003) doi: 10.1139/E02-063 Abstract:

Reisz, R.R., Laurin, M. and Marjanović, D. 2010. *Apsisaurus whitteri* from the Lower Permian of Texas: yet another small varanopid, not a diapsid. Journal of Vertebrate Paleontology, 30(5): 1628–1631.

Ricker, W.E. 1973. Linear regression in fishery research. Journal of Fishing Research Board of Canada 30:409–434.

Rieppel, O. and Reisz, R.R. 1999. The origin and early evolution of turtles. Annual Review of Ecology and Systematics 30: 1–22.

Romer, A.S. 1956. Osteology of the Reptiles. University Chicago Press. p. 1–772.

Romer, A.S. 1966. Vertebrate Paleontology, 3rd Edition. Chicago: University of Chicago Press. 687 pp.

Rossmann, T. 2000. Studien an Mesosauriern (Amniota inc. sed.: Mesosauridae): 2. Neue Erkenntnisse zur Anatomie, mit Berücksichtigung der Taxonomie von *Mesosaurus pleurogaster* (Seeley). Senckenbergiana lethaea 80(1): 13–28.

Rubenstein, N.M. 1971. Ontogenetic allometry in the salamander genus *Desmognathus*. American Midland Naturalist 85: 329–348.

Sanchez-Villagra, M.R. 2010. Developmental palaeontology in synapsids: the fossil record of ontogeny in mammals and their closest relatives. Proceedings of the Royal Society B: Biological Sciences, 277(1685): 1139–1147. doi:10.1098/rspb.2009.2005

Santos, R. V., Souza, P. A., de Alvarenga, C. J. S., Dantas, E.L., Pimentel, M.M., de Oliveira, C.G. and de Araújo, L.M. 2006. Shrimp U–Pb zircon dating and palynology of bentonitic layers from the Permian Irati Formation, Paraná Basin, Brazil. Gondwana research 9(4): 456–463.

Sears, K.E., Goswami, A., Flynn, J.J. and Niswander, L.A. 2007. The correlated evolution of Runx2 tandem repeats, transcriptional activity, and facial length in carnivora. Evolution & development 9 (6): 555–565.

Seeley, H.G. 1892. The Mesosauria of South Africa. Quarterly Journal of the Geological Society 48(1-4): 586–604.

Shikama, T. and Ozaki, H. 1966. On a reptilian skeleton from the Paleozoic formation of São Paulo, Brazil. Transaction Proceedings of the Paleontological Society of Japan 64: 351–358.

Shubin, N.H. and Alberch, P. 1986. A morphogenetic approach to the origin and basic organization of the tetrapod limb. Evolutionary Biology 20: 319–387.

Smith, R.J. 2009. Use and misuse of the reduced major axis for line fitting. American Journal of Physical Anthropology 140(3): 476–486.

Smithson TR. 1989. The earliest known reptile. Nature 342:676–677.

DOI 10.1038/342676a0.

Smithson RT, Carroll RL, Panchen AL, Andrews SM. 1994. Westlothiana lizziae from the Viséan of East Kirkton, West Lothian, Scotland, and the amniote stem. Transactions of the Royal Society of the Edinburgh, Earth Sciences 84:383–412. DOI 10.1017/S0263593300006192.

Snell, O. 1892. Die Abhängigkeit des Hirngewichts von dem Körpergewicht und den geistigen Fähigkeiten. Archives of Psychiatric Nursing 23(2): 436–446. doi:10.1007/BF01843462.

Stayton, C.T. 2015. What does convergent evolution mean? The interpretation of convergence and its implications in the search for limits to evolution. Interface Focus 5(6): 20150039. doi: 10.1098/rsfs.2015.0039

Sumida, S.S. 1989. Reinterpretation of vertebral structure in the Early Permian pelycosaur *Varanosaurus acutirostris* (Amniota: Synapsida). Journal of Vertebrate Paleontology 9 (4): 451–458.

Tarasoff, F.J., Bisaillon, A., Piérard, J. and Whitt, A.P. 1972. Locomotory patterns and external morphology of the river otter, sea otter, and harp seal (Mammalia). Canadian Journal of Zoology 50(7): 915–929.

Trujillo-Ortiz, A. and Hernandez-Walls, R. 2010. gmregress: Geometric Mean Regression (Reduced Major Axis Regression). A MATLAB file. [www document]. URL http://www.mathworks.com/matlabcentral/fileexchange/27918-gmregress

Tsuji, L.A and Müller, J. 2009. Assembling the history of the Parareptilia: phylogeny, diversification, and a new definition of the clade. Fossil Record 12: 71–81. doi:10.1002/mmng.200800011

Tsuji, L.A., Müller, J. and Reisz, R.R. 2012. Anatomy of *Emeroleter levis* and the phylogeny of the nycteroleter parareptiles. Journal of Vertebrate Paleontology 32: 45–67.doi: 10.1080/02724634.2012.626004

Vaughn, P.P. 1962. The Paleozoic Microsaurs as close relatives of reptiles, again. The American Midland Naturalist 67: 79–84.

Villamil, J., Núñez Demarco, P., Meneghel, M., Blanco, R.E., Jones, W., Rinderknecht, A., Laurin, M. and Piñeiro, G. 2015. Optimal swimming speed estimates in the Early Permian mesosaurid *Mesosaurus tenuidens* Gervais, 1865 from Uruguay. Historical Biology 28: 963–971. doi: 10.1080/08912963.2015.1075018

Wegener, A. 1966. The Origin of Continents and Oceans. 246 pp. Dover Publications, Inc.,New York [English translation of the German 4th edition, from 1929].

Young, N.M., Winslow, B., Takkellapati, S. and Kavanagh, K. 2015. Shared rules of development predict patterns of evolution in vertebrate segmentation. Nature communications 6(1): 1–7.

Zhao, Q., Benton, M.J., Xu, X., and Sander, P.M. 2014. Juvenile-only clusters and behaviour of the Early Cretaceous dinosaur *Psittacosaurus*. Acta Palaeontologica Polonica 59 (4): 827–833.

Zar J. 1999. Biostatistical analysis. 4th ed. Upper Saddle River, NJ: Prentice Hall, Upper Saddle River, New Jersey, 931 pp.

Table 1

Download source file (13.88 kB)

ACTA PALAEONTOLOGICA POLONICA

Table 1. Statistical results for the log data resampled 100000 times: mean of the coefficient *a*, its 95% confiden mean correlation coefficient, percentage of resampled set that include 1 in its confidence interval (i.e. that are is SkL-SnL: Skull length minus snouth length. PBO-PBS: length between the posterior border of orbit and the pos of the skull. CI-CV: Metacarpals. TI-TV: Metatarsals.

	a	*0.95% Confidence interval*		Mean correlation coefficient	resampling % that include 1
		lower	*upper*		
Skull					
Snout width:Skull length	0.8771	0.6049	1.3453	0.9045	88.6%
Snout length:Skull length	1.0818	0.2477	2.0684	0.9898	99.9%
SkL-SnL:Skull length	1.49	-1.1931	2.5689	0.9642	100%
Orbit length:Skull length	0.7426	0.3039	1.2535	0.8413	41.1%
PBO-PBS length:Skull length	0.9695	0.414	1.6734	0.8403	93.8%
maximum Skull width:Skull length	0.8711	-0.8682	1.5011	0.923	88%
maximum width:Orbit length	1.3738	0.7341	2.3662	0.961	100%
Femur					
length:proximal width	0.8548	0.2119	1.5643	0.7356	99.8%
length:central width	0.8578	0.1487	1.6157	0.738	100%
length:distal width	0.8111	0.1957	1.4778	0.7592	99.5%
Fibula					
length:proximal width	1.161	0.2039	2.1885	0.8706	100%
length:central width	0.9329	0.2142	1.72	0.8337	100%
length:distal width	1.1861	0.227	2.2155	0.9352	100%
Tibia					
length:proximal width	1.1166	0.2638	2.0526	0.7718	100%
length:central width	1.1195	0.2807	2.0396	0.742	100%
length:distal width	0.940	0.297	1.670	0.6806	99.9%
Astragalus					
length:proximal width	0.8006	0.1711	1.473	0.8495	5%
length:central width	0.8029	0.1981	1.456	0.8143	32%
length:distal width	0.981	0.2788	1.7735	0.8612	98%
Calcaneus					
length:width	1.0487	0.3311	1.865	0.8998	100%
Humero					
length:proximal width	0.9668	0.3122	1.7118	0.7517	99.9%
length:central width	0.8273	0.1973	1.5155	0.8748	100%
length:distal width	0.9458	0.1536	2.0311	0.9458	100%
Radius					
length:proximal width	1.0575	0.3328	1.9086	0.8624	99.9%
length:central width	1.1271	0.2685	2.0626	0.8786	100%
length:distal width	0.9638	0.2201	1.784	0.8838	100%
Ulna					
length:proximal width	1.2063	0.4223	2.1444	0.8829	100%
length:central width	0.9868	0.3661	1.7274	0.8458	100%
length:distal width	1.0994	0.3166	1.978	0.8912	100%

Table 1

Download source file (13.88 kB)

ACTA PALAEONTOLOGICA POLONICA

Relationship between bones' length

Femur:Tibia	0.9262	0.0632	1.8036	0.9839	50%
Femur:Fibula	0.9477	0.0877	1.8346	0.972	63%
Femur:TI	1.1285	0.1898	2.1355	0.9375	100%
Femur:TII	1.0598	0.1971	1.9779	0.9563	99.9%
Femur:TIII	1.0436	0.1573	1.974	0.9693	99.9%
Femur:TIV	1.039	0.1933	1.9425	0.9668	99.5%
Femur:TV	1.1097	0.2247	2.0439	0.9658	100%
Femur:Astragalus	1.5563	0.4775	2.7803	0.8542	100%
Femur:Humerus	0.9108	0.1776	1.7006	0.9019	100%
Humerus:Ulna	0.9136	0.1222	1.7402	0.9728	50%
Humerus:Radius	0.9229	0.1319	1.7505	0.968	52%
Humerus:CI	1.0431	0.3565	1.8352	0.9347	99.9%
Humerus:CII	0.8929	0.2113	1.6751	0.9427	97.9%
Humerus:CIII	0.9183	0.2263	1.6727	0.9379	37%
Humerus:CIV	0.8013	0.2828	1.4178	0.9232	60.0%
Humerus:CV	0.8755	0.3975	1.4921	0.8364	37.9%
Femur+Tibia:TI	0.5748	0.1	1.086	0.9413	99.9%
Femur+Tibia:TV	0.5729	0.1139	1.0515	0.973	66.80%
Humerus+Radio:CI	0.5585	0.2189	0.9823	0.939	98.10%
Humerus+Radio:CV	0.4643	0.2199	0.7969	0.85	19.30%
Skull length:Mean vertebral length	1.4561	-0.0597	2.3553	0.7119	99.9%
Femur length:Mean vertebral length	1.0171	0.2499	1.8745	0.8773	99.9%
Femur length:Skull length	1.5472	0.9031	2.4602	0.7908	100%
Humerus length:Skull length	1.472	-0.9549	2.4054	0.6987	100%

ce interval,
sometric).
terior border

interpretation

Isometric
Isometric
Isometric
Isometric
Isometric
Isometric
Isometric

Isometric
Isometric
Isometric

Isometric
Isometric
Isometric

Isometric
Isometric
Isometric

Isometric
Isometric
Isometric

Isometric

Isometric
Isometric
Isometric

Isometric
Isometric
Isometric

Isometric
Isometric
Isometric

Table 1

Download source file (13.88 kB)

Isometric
Isometric
Isometric
Isometric
Isometric
Isometric
Isometric
Isometric
Isometric
Isometric
Isometric
Isometric
Isometric
Isometric
Isometric
Isometric

Isometric
Isometric
Allometric (-)
Allometric (-)

Isometric
Isometric
Isometric
Isometric

ACTA PALAEONTOLOGICA POLONICA

Table 2. Historical review of the available literature where the structure of the mesosaur carpus was suggested. The three previously proposed mesosaur taxa are included to show that despite the disparity in the bone identification, there is a common pattern that depends on the degree of ossification and fusion of elements (i.e. ontogenetic stages). Small elements as the pisiforme and distal tarsal V can be lost. Text marked in orange refers to data obtained in the present study.

	Mesosaurus	*Stereosternum*	*Brazilosaurus*	References
Intermedium	Present	Present	Present	Huene (1941); Kuhn (1969); Seeley (1892); Mac Gregor (1908); Modesto (1996); Rossmann (2000);
	Present			**This paper**
Radiale	Present or unossified	unossified	unossified	Gervais (1865); Mac Gregor (1908); Modesto (1996); this paper
	Present, unossified or fused to centrale			**This paper**
Ulnare	Present	Present	Present	Huene (1941); Kuhn (1969); Seeley (1892); Mac Gregor (1908); Rossmann (2000)
	Present			**This paper**
Centrale	Present	Present	Present	Seeley (1892); Modesto (1996); Rossmann (2000)
	Present			**This paper**
Medial centrale	–	Present, unossified or absent	–	Modesto (1996; 2010)
	Probably present and fused with central			**This paper**
Pisiform	–	Present	?Present	Gervais (1865), Seeley (1892); Modesto (1996);
	Present			**This paper**
Number of Distal Tarsals	4			Gervais (1865); Huene (1941); Kuhn (1941); Seeley (1892); Mac Gregor (1908);
	5	**5**	4	Modesto (1996); Rossmann (2000)
	5, fifth ossify later			**This paper**
Largest Distal Tarsal	First, First, Fourth; first; first	–	–	Huene (1941), Kuhn (1969); Seeley (1892); Mac Gregor (1908); Modesto (1996)
	Variable			**This paper**

Figure 1

Download source file (922.87 kB)

ACTA PALAEONTOLOGICA POLONICA

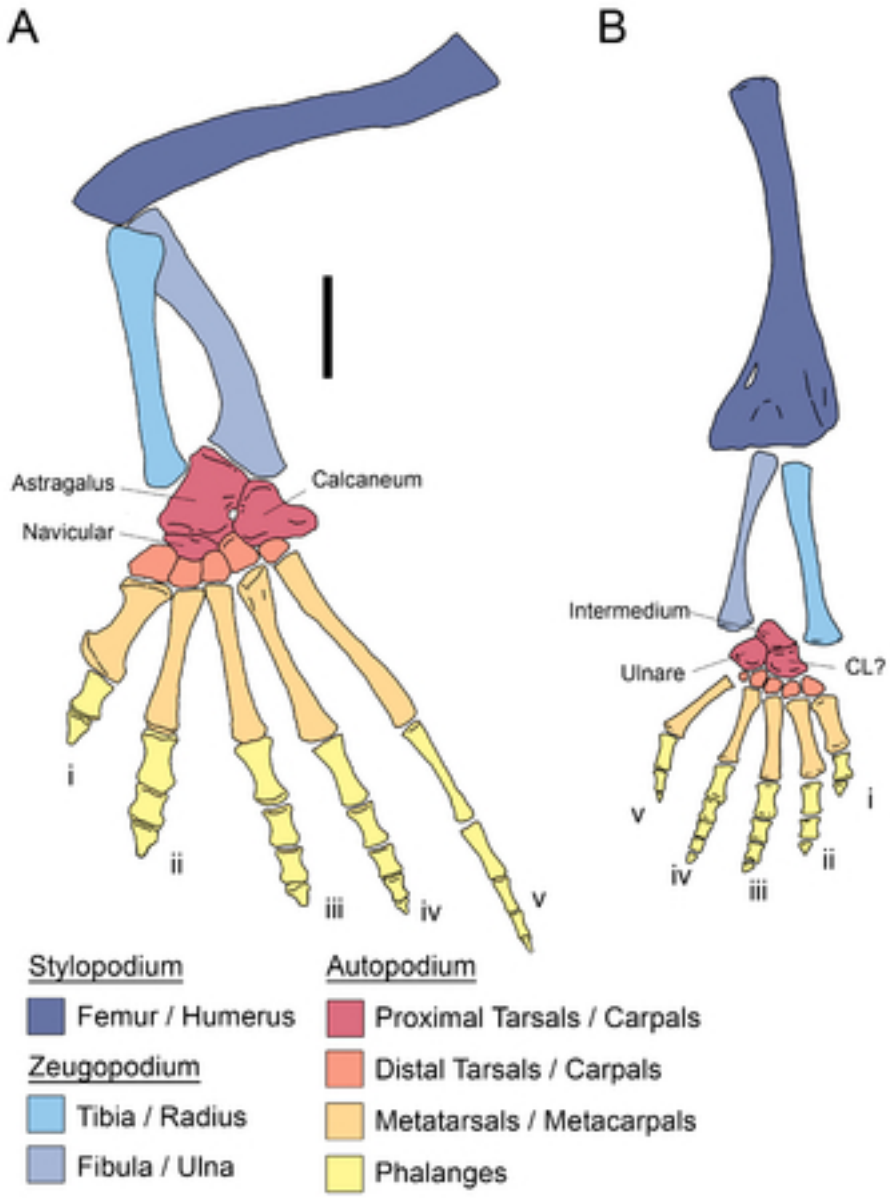

Figure 1. Anatomical reconstruction of (A) pes / hindlimb and (B) manus / forelimb in an adult Mesosaurus tenuidens. Colours indicate the identity of the different elements that form the limbs. Scale bar: 10 mm. (CL?): Lateral Centrale? (ontogenetic development of this bone is discussed in detail in the carpus section), i-v finger/toe numbers. Modified from Piñeiro et al. (2016).

ACTA PALAEONTOLOGICA POLONICA

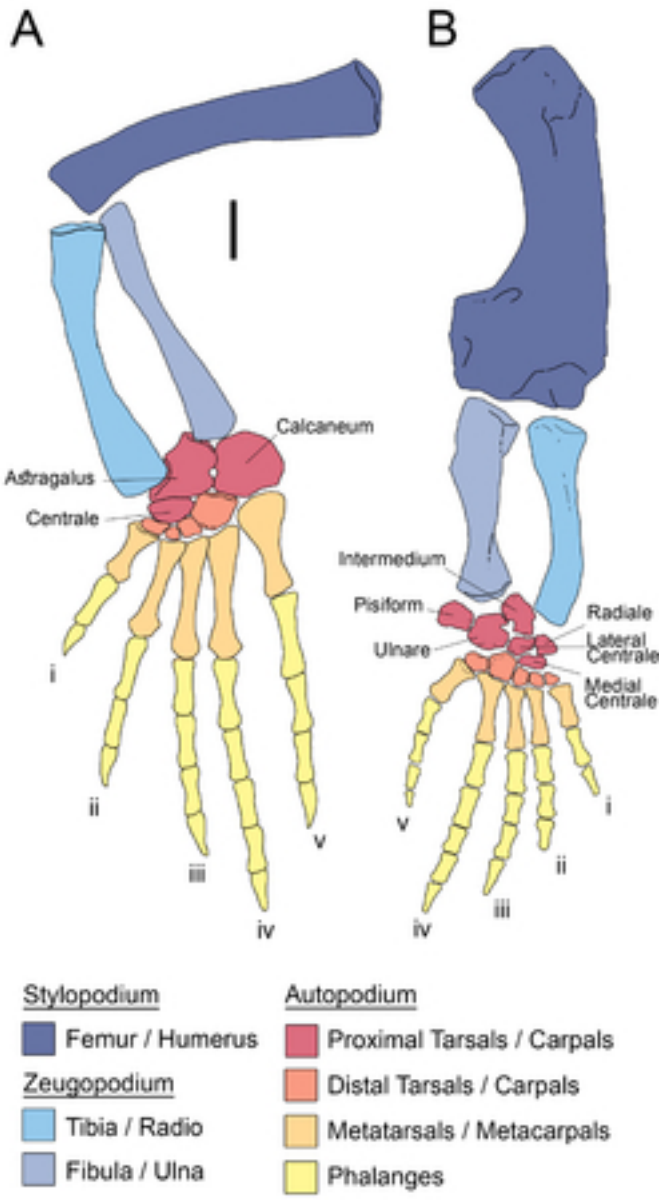

Figure 2. Anatomical reconstruction of (A) pes / hindlimb and (B) manus / forelimb in an adult Hovasaurus boulei. Colours indicate the identity of the different elements that form the limbs. i-v finger/toe number. Scale bar: 10 mm. Based in Currie (1981) and Caldwell (1997).

Figure 3

[Download source file (774.55 kB)]

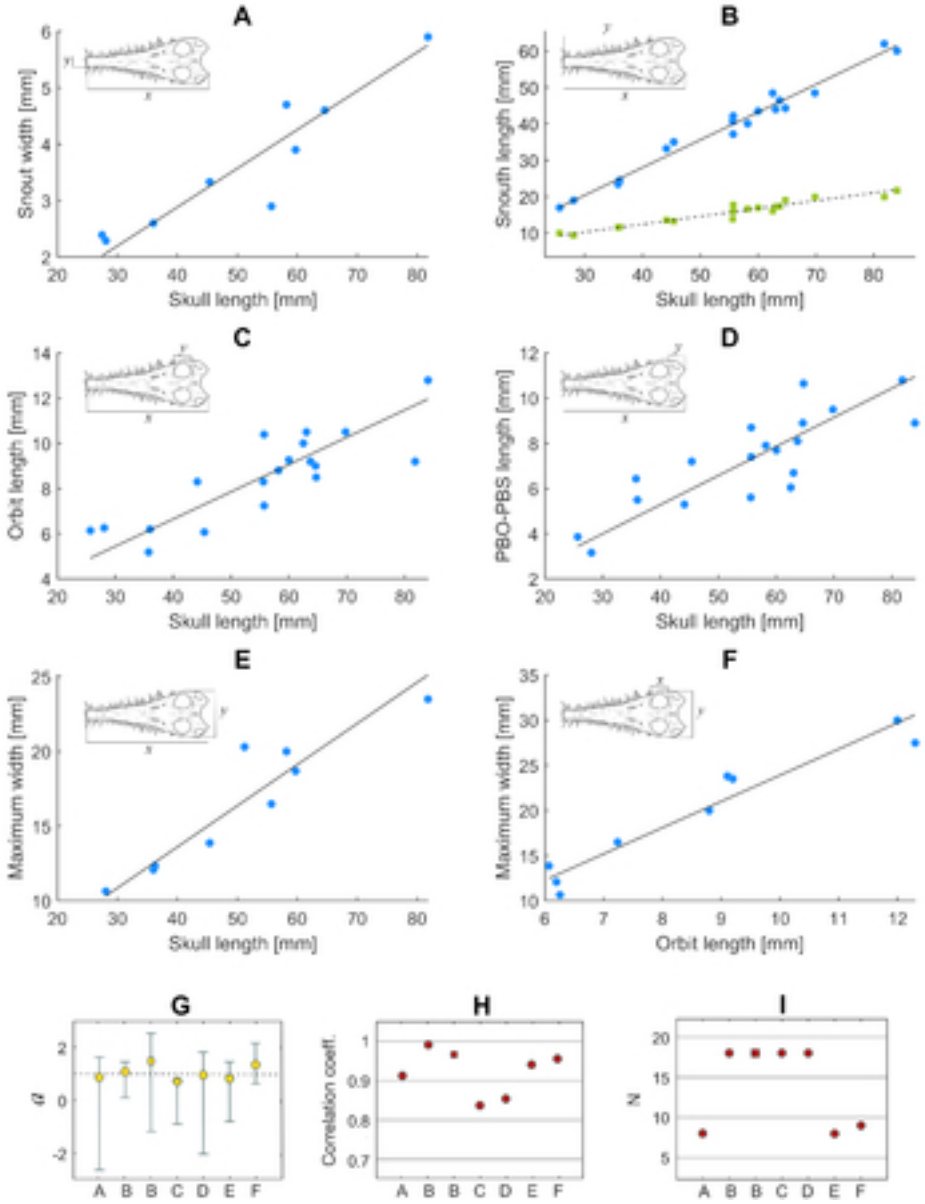

Figure 3. Relationships found in different regions of the mesosaur skull. (A-F) linear relationships between different elements of the mesosaur skull. (B): skull length against snout length (circles); skull length against “skull length minus snout length” (squares) PBO-PBS: length between the posterior border of orbit and the posterior border of the skull. The measured regions are indicated in the upper left corner of each figure; x and y indicate the axis on which the measurement is plotted. (G-I) shows the respective statistical parameters: (G) Coefficient a and its 95% confidence interval, (H) Correlation coefficient. (I) Number of samples.

Figure 4

Download source file (181.25 kB)

ACTA PALAEONTOLOGICA POLONICA

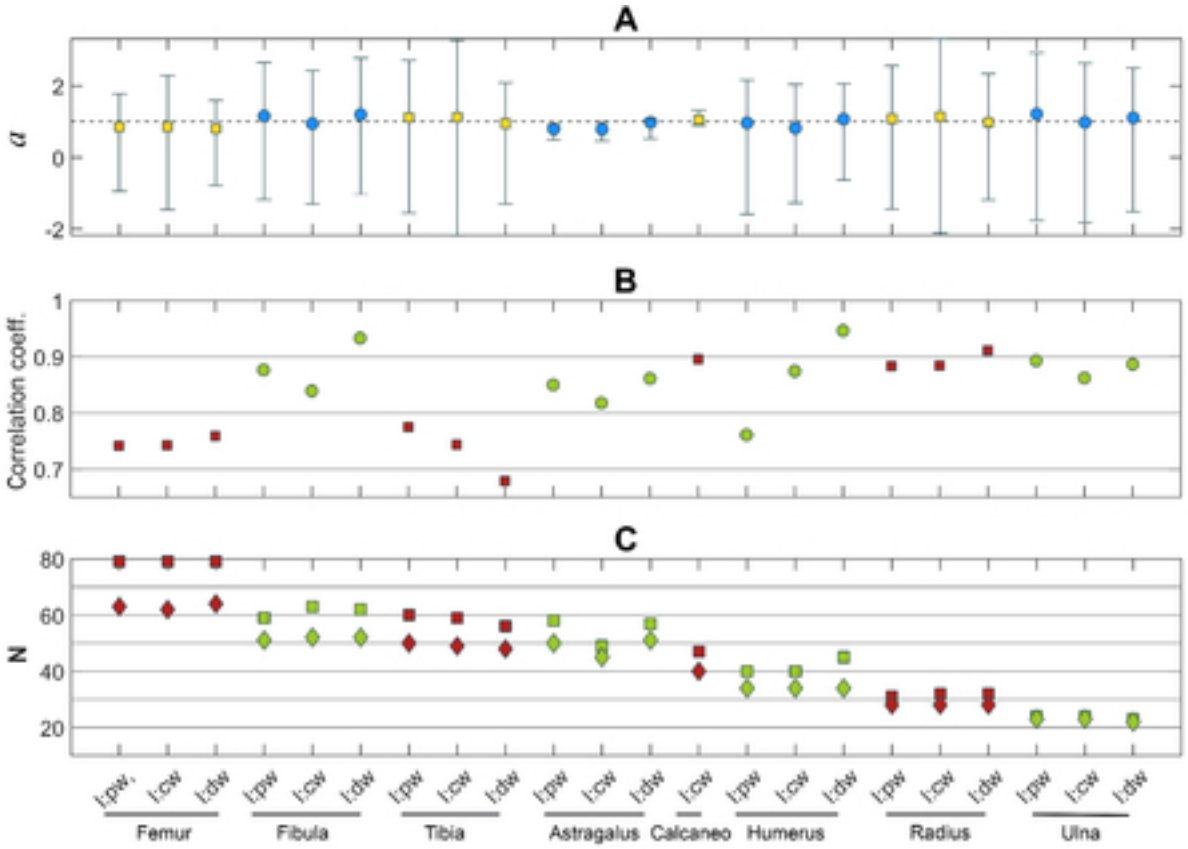

Figure 4. Resultant parameters from the comparison between length and width of different limb bones of Mesosaurus. (A) Coefficient a and its 95% confidence interval, (B) Correlation coefficient. (C) Number of measurements/samples (squares) and number of individuals (diamonds) studied. Acronyms: l: length, pw: proximal width, cw: central width, dw: distal width.

ACTA PALAEONTOLOGICA POLONICA

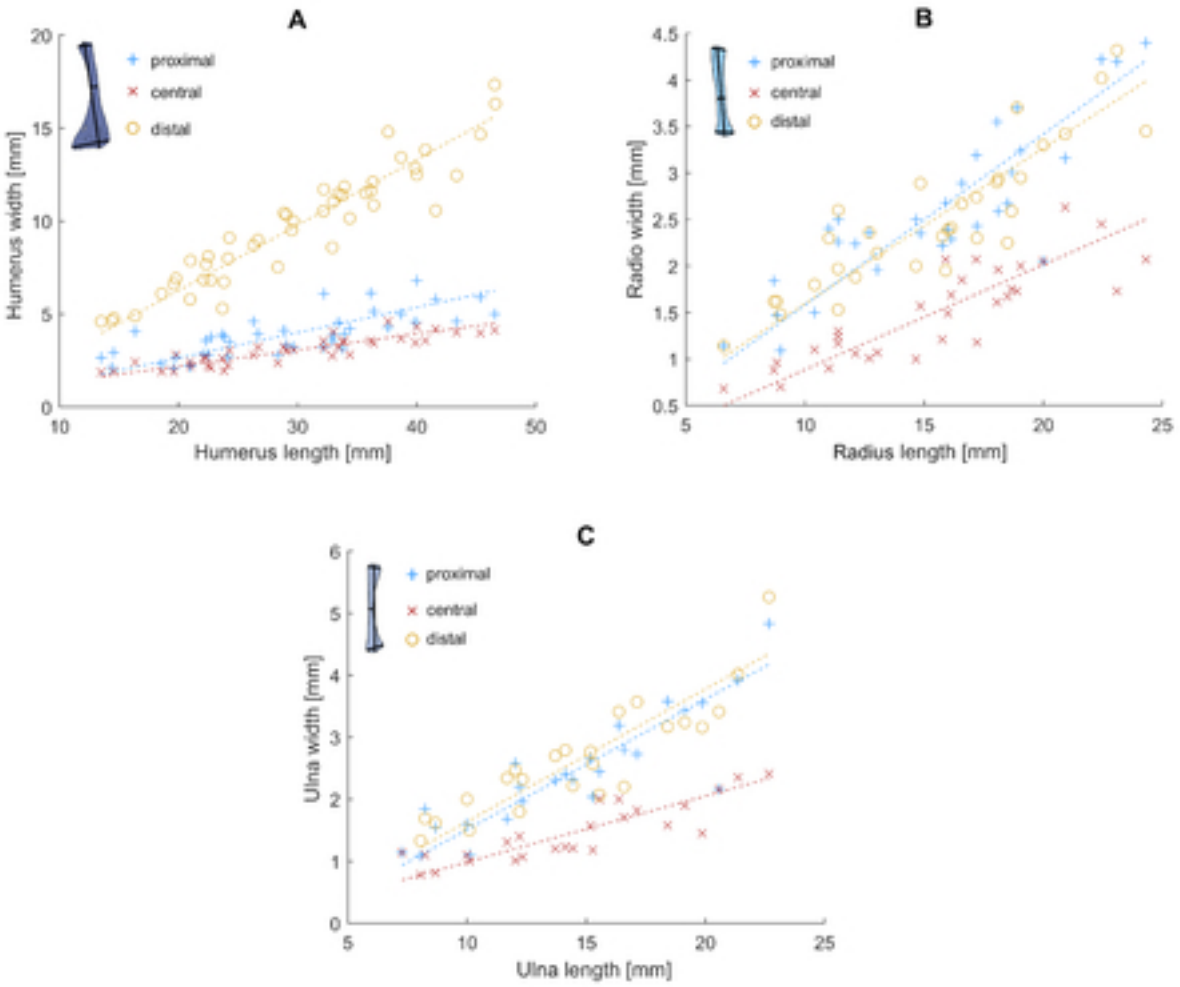

Figure 5. Length vs. width relationships in different forelimb bones of mesosaurs. A-C. The measured bone and the measurements taken are indicated in the upper left corner of each figure (see Fig. 1). Proximal (+), medial (x) and distal (o) bone width. The statistical parameters are indicated in Fig. 4.

ACTA PALAEONTOLOGICA POLONICA

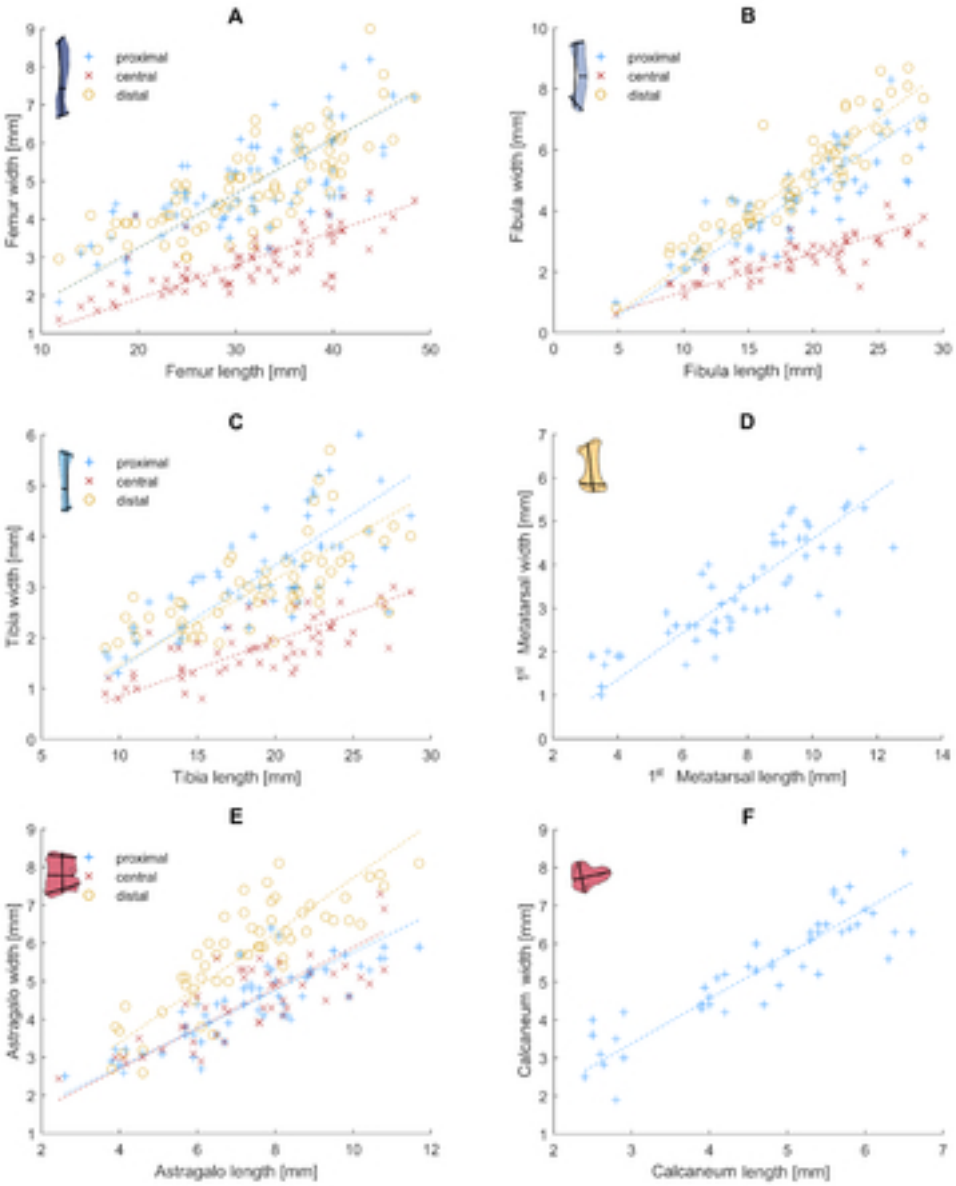

Figure 6. Length vs. width relationships in different hindlimb bones of mesosaurs. A-E. The measured bone and the measurements taken are indicated in the upper left corner of each figure (see Fig. 1). Proximal (+), medial (x) and distal (o) bone width. Statistical parameters are indicated in Fig. 4.

Figure 7

Download source file (174.3 kB)

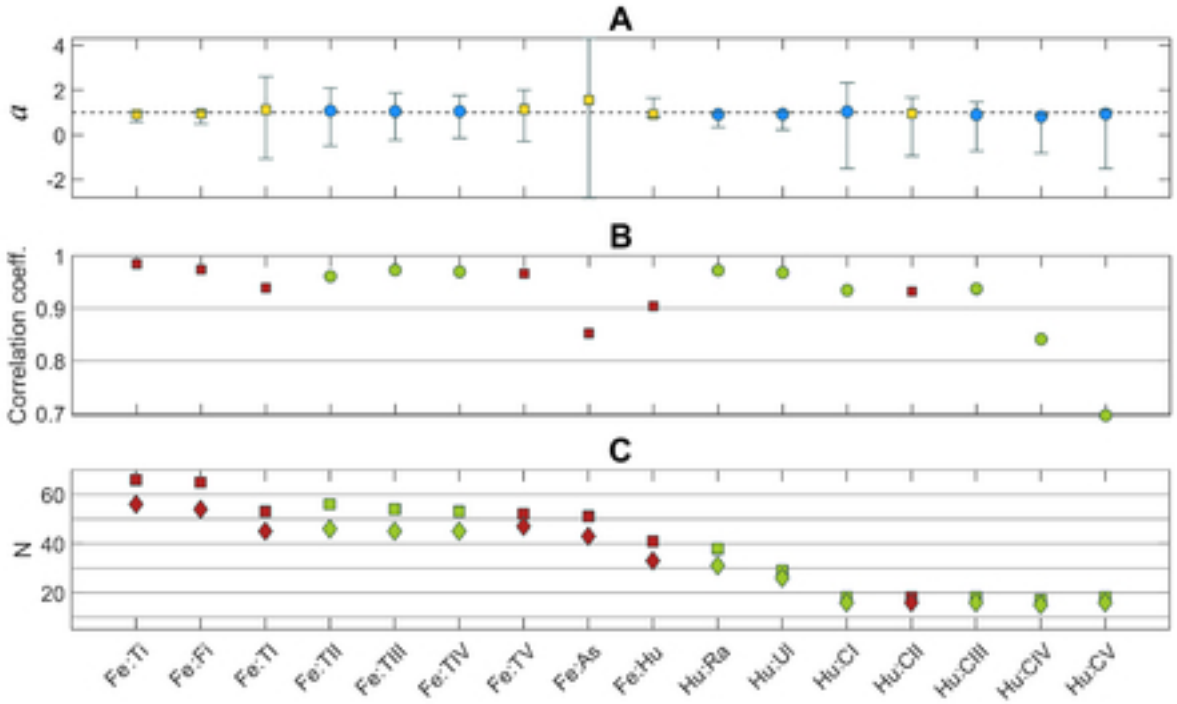

Figure 7. Resultant parameters from comparison between the length of different mesosaur limb bones. (A): Coefficient a and its 95% confidence interval. (B): Correlation coefficient. (C): Number of measurements/samples (squares) and number of individuals (diamonds) studied. Acronyms: As: Astragalus, CI-CV: Metacarpals, Fe: Femur, Fi: Fibula, Hu: Humerus, Ra: Radius, Ti: Tibia, TI-TV: Metatarsals, Ul: Ulna.

Figure 8

[Download source file (1.69 MB)]

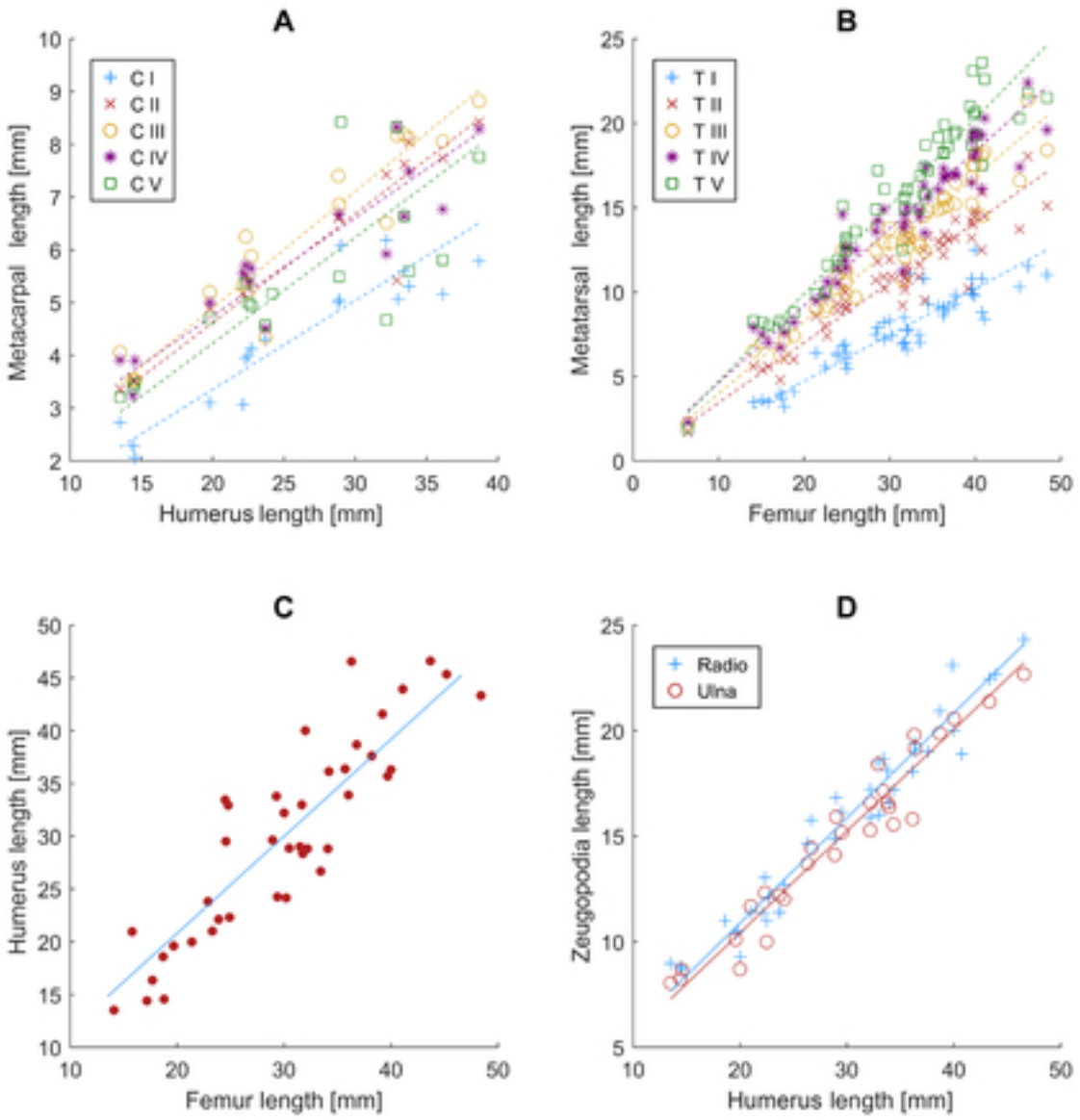

Relationship between the lengths of different mesosaur forelimb and hindlimb bones. The respective statistical parameters are provided in Fig. 7. CI-CV: Metacarpals, TI-TV: Metatarsals.

ACTA PALAEONTOLOGICA POLONICA

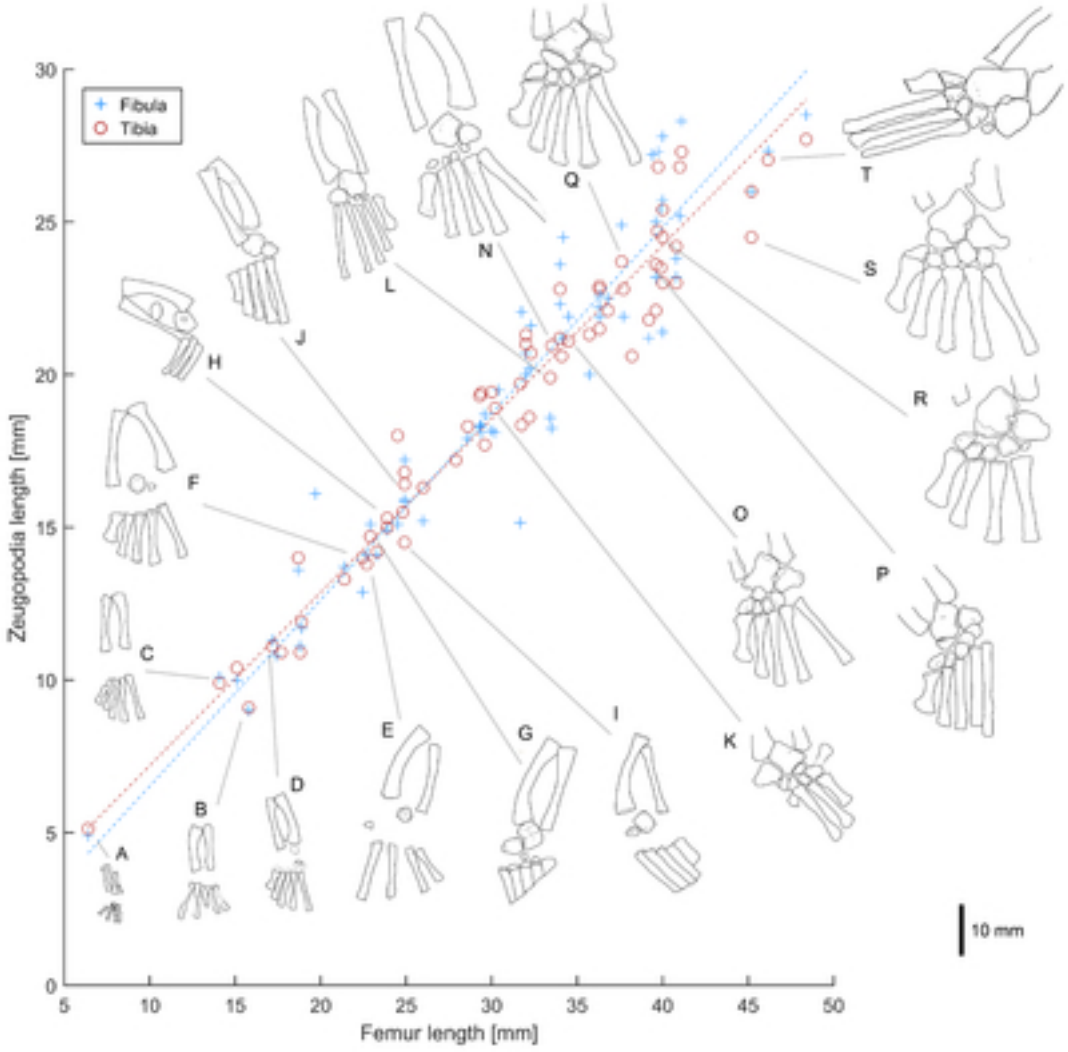

Figure 9. Lengths of femora vs. zeugopodia in mesosaurs. Blue plus signs: fibulae measurements; Red circles: tibiae measurements. Statistical parameters are shown in Fig. 7. A-T: Tarsal ontogeny of embryonic to adult mesosaurs illustrated following Piñeiro et al. (2016), see also Fig. 12. A: FC-DPV 2504; B:AMNH 23799; C:SMF-R4513-young; D: GP-2E 272; E: AMNH 23795; F: SMF-R 4496; G: SMF-R 4513-older; H: SMF-R 4934; I: MN 4741; J:PIMUZ A-III 591; K: GP-2E 114; L:GP/2E 6519-E; N: GP/2E 6519-A; O: SMF-R 4470; P: SMF-R 4528; Q: GP-2E 657b; R: FC-DPV 2058; S: GP-2E 5740; T:SMF-R 4477. Specimens A, D-I, K, M, O-S were previously analysed by Piñeiro et al. (2016).

Figure 10

Download source file (1.86 MB)

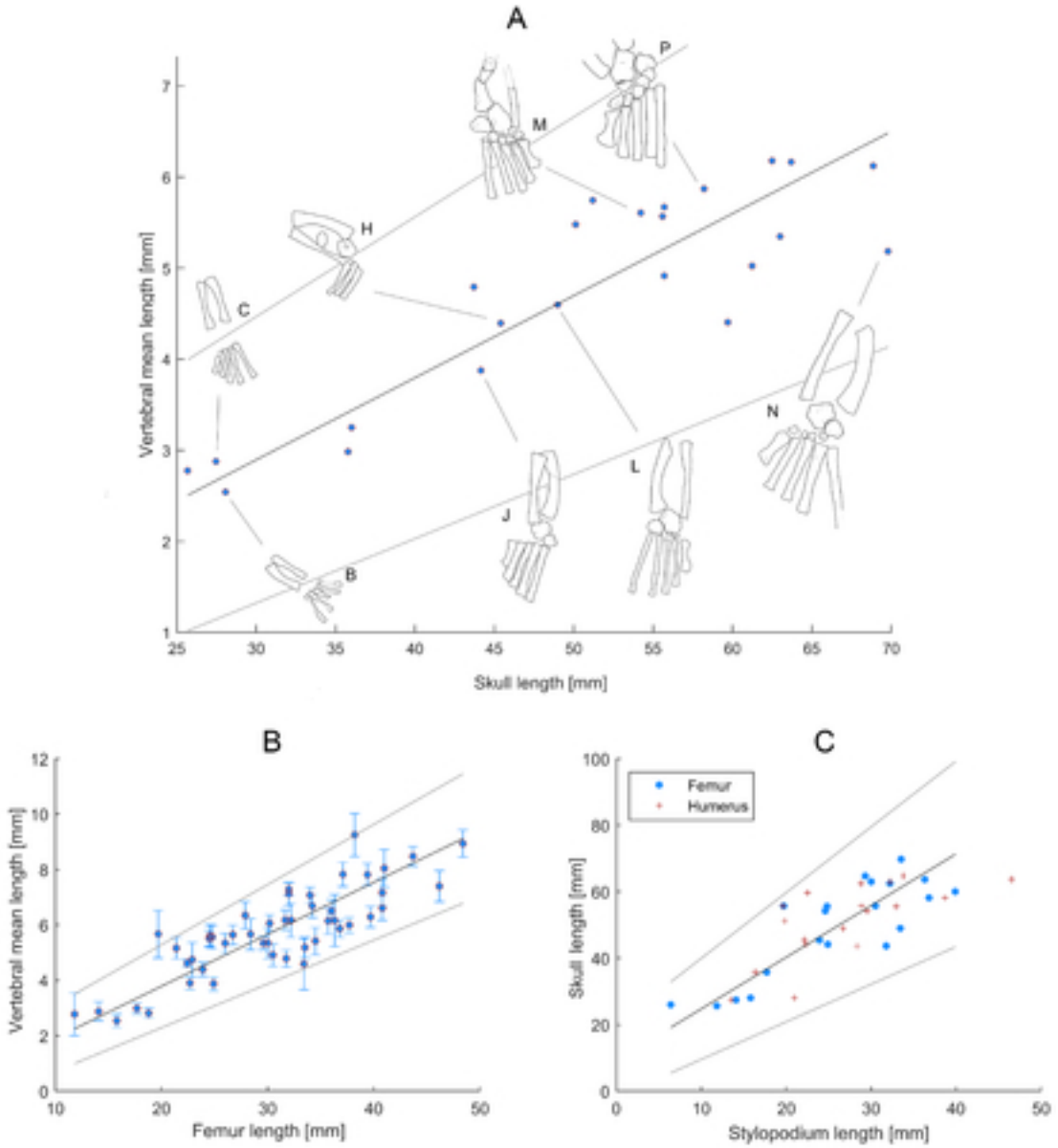

Figure 10. Relationships between skull length, vertebral mean length and stylopodium length in mesosaurs. (A): Relationship between skull length and vertebral mean length. Ontogenetic stage of the specimens is illustrated following Piñeiro et al. (2016), see also Fig. 12. B:AMNH 23799; C:SMF-R4513-young; H: SMF-R 4934; J:PIMUZ A-III 591; L:GP/2E 6519-E; M: PF IPL 220011/04 770; N: GP/2E 6519-A; P: SMF-R 4528; Specimens H, M, P were previously analysed by Piñeiro et al. (2016). (B): Relationship between femur length and vertebral mean length with its 3σ interval. (C): Relationship between skull length, and zeugopodial length in mesosaurs. 95% confidence interval is shown in each plot.

Figure 11

Download source file (8.22 MB)

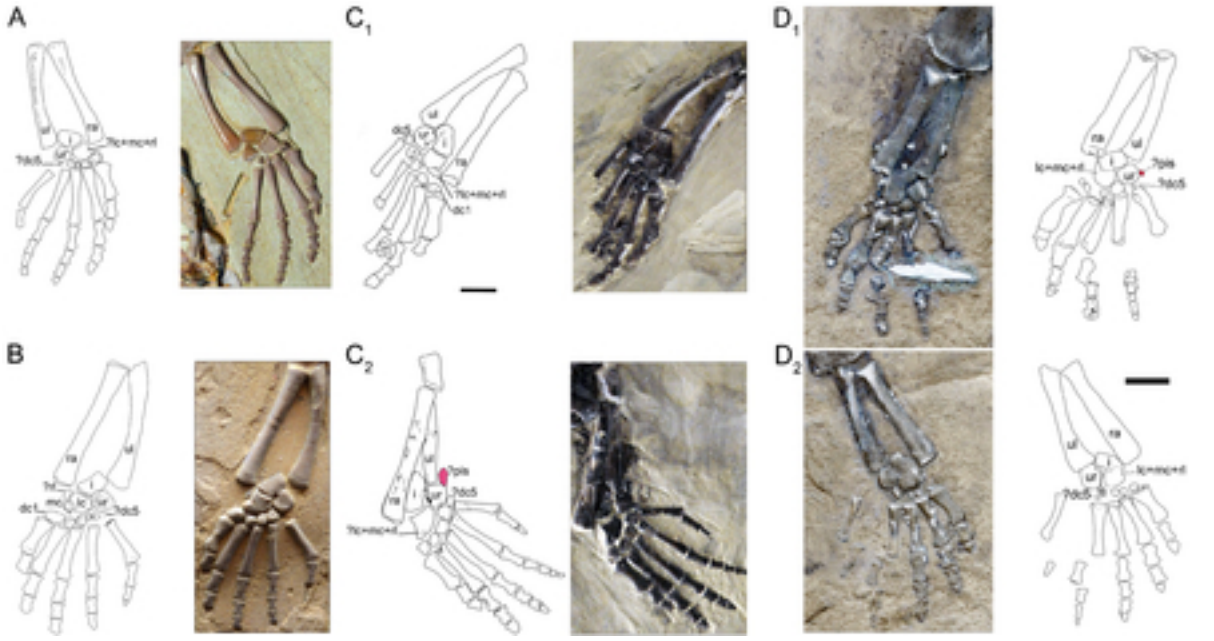

Figure 11. Structure of the mesosaur carpus in presumed subadult and adult specimens. (A-B): Photographs and interpretive drawings of manus of sub-adult or young adult mesosaur specimens (SMF-R 4492 and 4528 respectively). In B, five bones can be seen in the proximal carpal series, including a small ossified radiale close to the lateral centrale. Four bones (and perhaps an incipiently ossified very small distal V) are preserved in the distal series. (C1-C2):, Interpretive drawings and photographs of right and left manus respectively of SMF-R 4710, a more mature specimen, which has only three bones in the proximal series, after the fusion of radiale, lateral centrale, and probably the medial centrale. There are five bones in the distal series, but the fifth continue to be the smallest. A small pisiforme can be seen in (C2). (D1-D2): Interpretive drawings and photographs of left and right manus of MNHN AC 1865-77A, the type specimen of Mesosaurus tenuidens Gervais, 1865, a mature mesosaur specimen showing the incipient fusion of intermedium and centralia plus radiale complex. A pisiforme and a distal tarsal V could have been present but were lost or are not well-preserved. Abbreviations: lc. lateral centrale; mc. medial centrale; i. intermedium; pis, pisiform; rl, radiale; ra, radius, ul, ulna; ur, ulnare. Scale bars: 5 mm.

Figure 12

Download source file (1.48 MB)

ACTA PALAEONTOLOGICA POLONICA

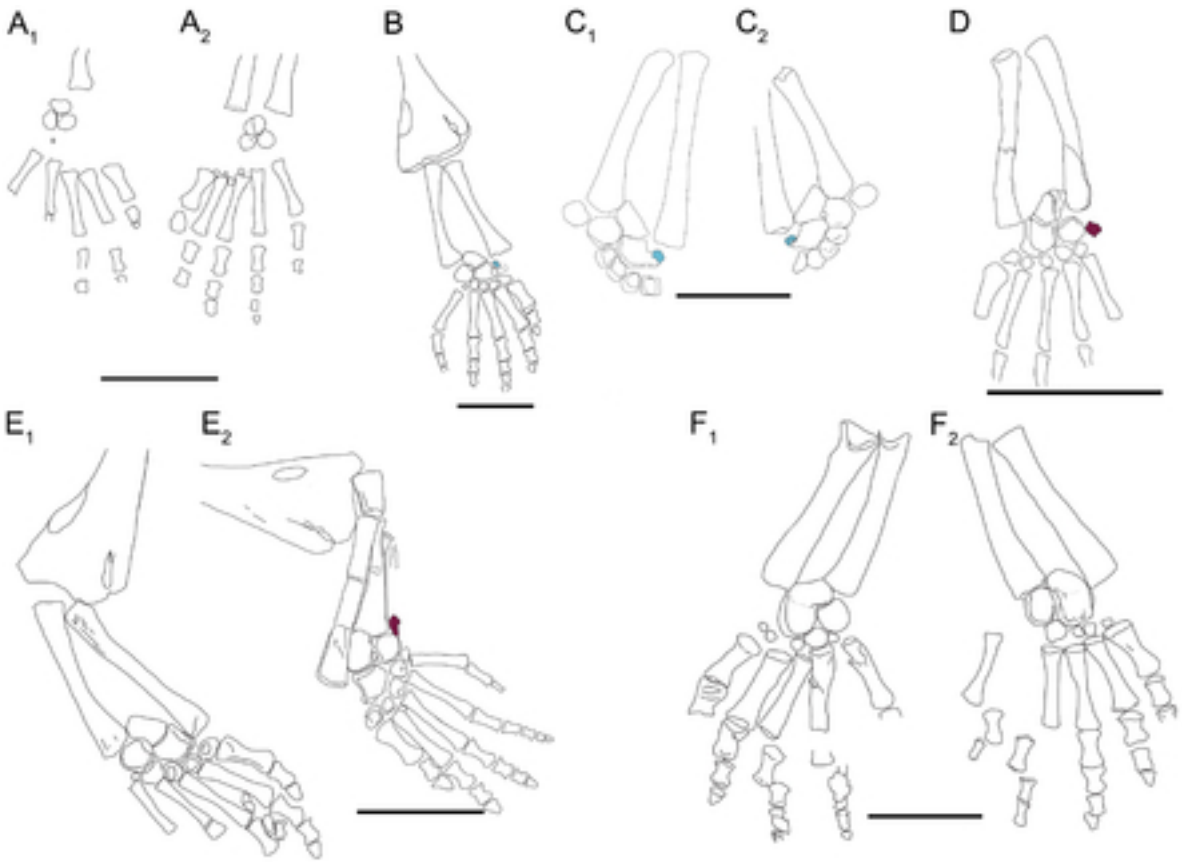

Figure 12. Variation of the mesosaur carpus structure through the growth. (A1-A2): Interpretive drawing of SMF-R 4485, left and right manus of a very immature individual, where just three rounded, featureless bones (intermedium, ulnare and possible lateral centrale) are present in the carpus. (B): Interpretive drawing of SMF-R 4528, specimen showing the most common carpus structure found in the available materials, where the intermedium and the centralia complex place closer together to finally fuse each other. A small radiale is still present (in light blue color). (C1-C2): Interpretive drawing of MCN-PV 2238A and B, part and counterpart of left manus showing the radiale (in light blue color) close to completing its fusion to the centralia. (D): Interpretive drawing of MN 7148 showing a more mature carpus and a small possible pisiforme (in dark red) present close to the ulnare carpal bone. (E1-E2): Interpretive drawing of SMF-R 4710, right and left manus of an adult mesosaur with the intermedium and the centralia plus radiale complex yet not fused. A small possible pisiform (in dark red) is present only in the right manus and absent from the left. (F1-F2): Interpretive drawing of MNHN AC 1865-77A, partial right and left forelimbs and manus of the type specimen of Mesosaurus tenuidens Gervais, 1865, where an incipient fusion of the intermedium with the centralia plus radial complex can be observed. There seem to be five distal tarsals although the fifth is indeed very small. Also, there can be a pisiforme, but the hands in this specimen have been exposed to partial degradation by the action of scavengers that damaged some of the smallest bones. Scale bars: 10 mm.

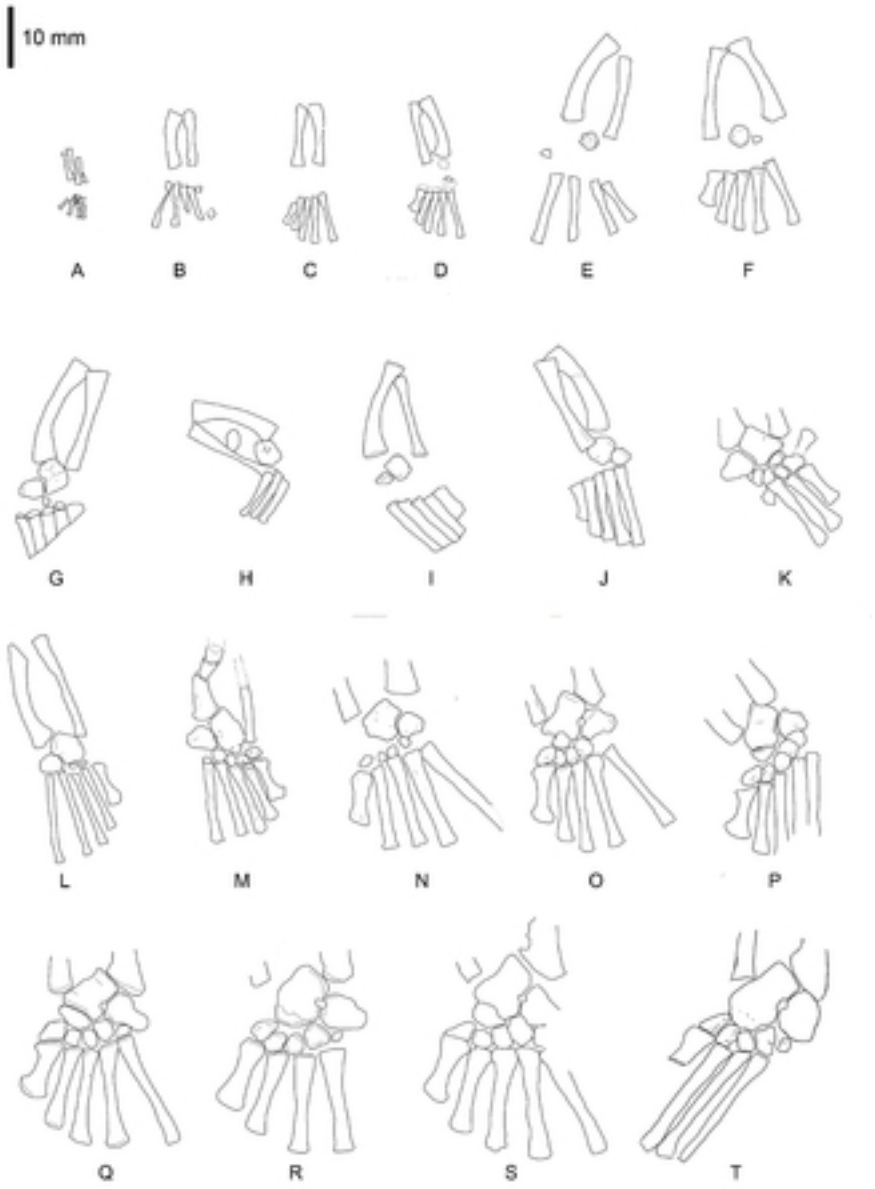

Figure 13. Mesosaurus tenuidens, ontogenetic transformation in the tarsus formation (after Piñeiro et al. 2016). A-T: Drawings of the selected specimens preserving epipodial, mesopodial and metapodial elements. SA: FC-DPV 2504; B:AMNH 23799; C:SMF-R4513-young; D: GP-2E 272; E: AMNH 23795; F: SMF-R 4496; G: SMF-R 4513-older; H: SMF-R 4934; I: MN 4741; J:PIMUZ A-III 591; K: GP-2E 114; L:GP/2E 6519-E; M: PF IPL 220011/04 770; N: GP/2E 6519-A; O: SMF-R 4470; P: SMF-R 4528; Q: GP-2E 657b; R: FC-DPV 2058; S: GP-2E 5740; T:SMF-R 4477. Specimens A, D-I, K, M, O-S were previously analysed by Piñeiro et al. (2016).

Figure 14

Download source file (679.09 kB)

ACTA PALAEONTOLOGICA POLONICA

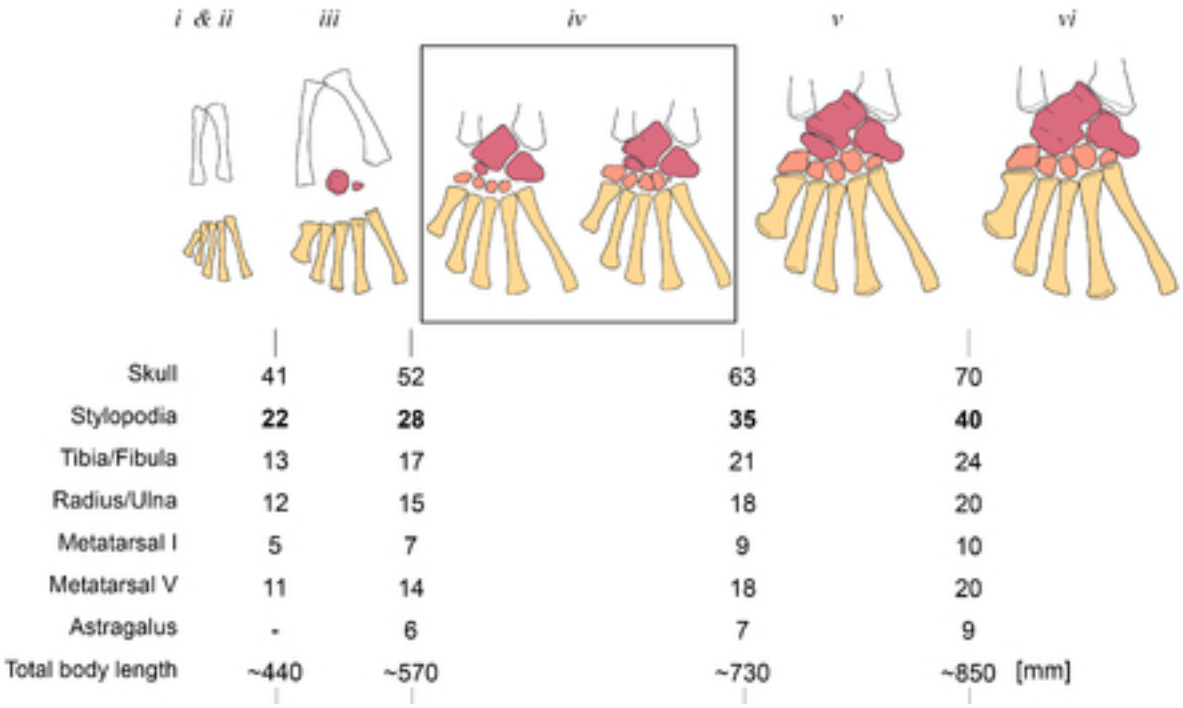

Figure 14. Schematic diagram of the ontogenetic transformation of the Mesosaurus tenuidens tarsus. Five stages are divided according to the ossification of the astragalus, calcaneum and navicular. Distal tarsal morphology can display some variations regarding the degree of ossification of the constituent bones (see the text). The approximate sizes (in millimetres) that the different elements would have in the transition between each category are tabulated according to our observations.

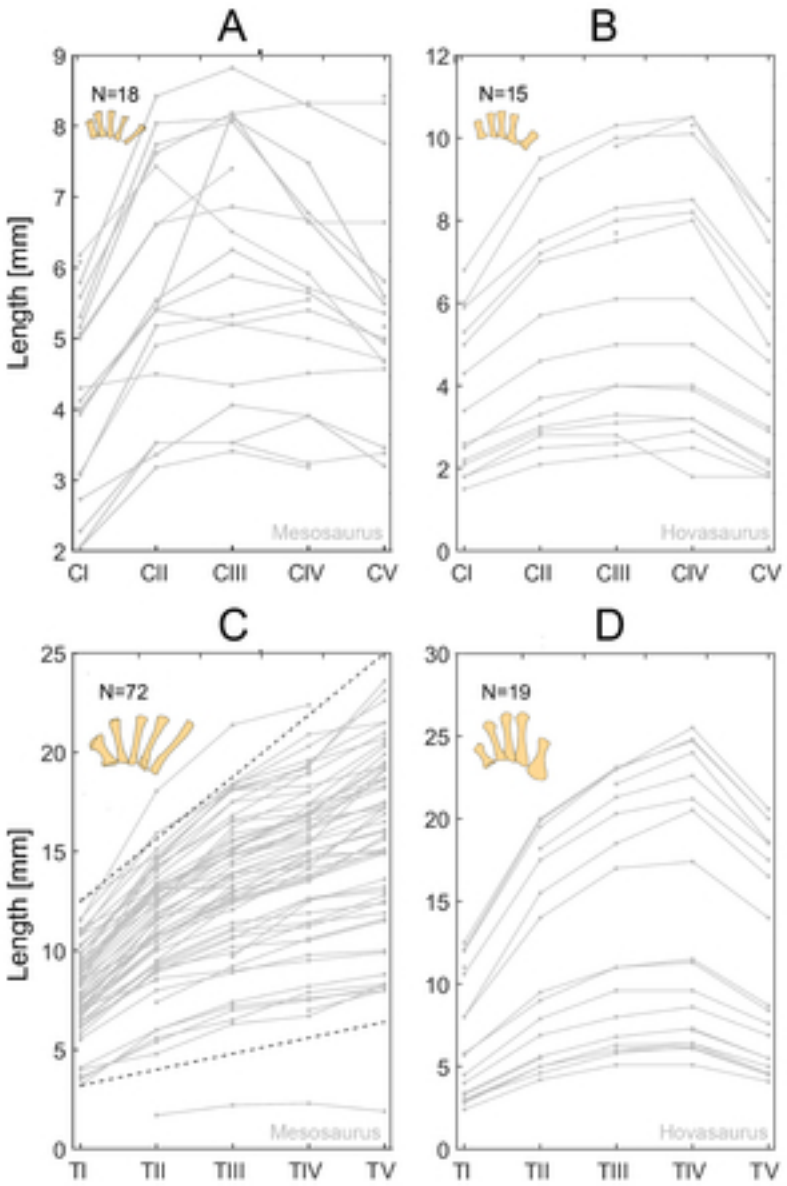

Figure 15. Metacarpal length measured in each Mesosaurus (A) and Hovasaurus (B) manus. Metatarsal lengths measured in each mesosaur (C) and Hovasaurus (D) pes. Each line represents the hand or foot of one specimen. Number of samples (N) is shown in each figure. Black dotted line represents the empirical proportions followed for the mesosaur metatarsals: mt(n)=mt(1)+n/4 where mt(1) is the measure of the first metatarsal. Metapodium is represented in the upper left corner of each figure (see Figs. 1, 2).

Figure 16

Download source file (3.22 MB)

ACTA PALAEONTOLOGICA POLONICA

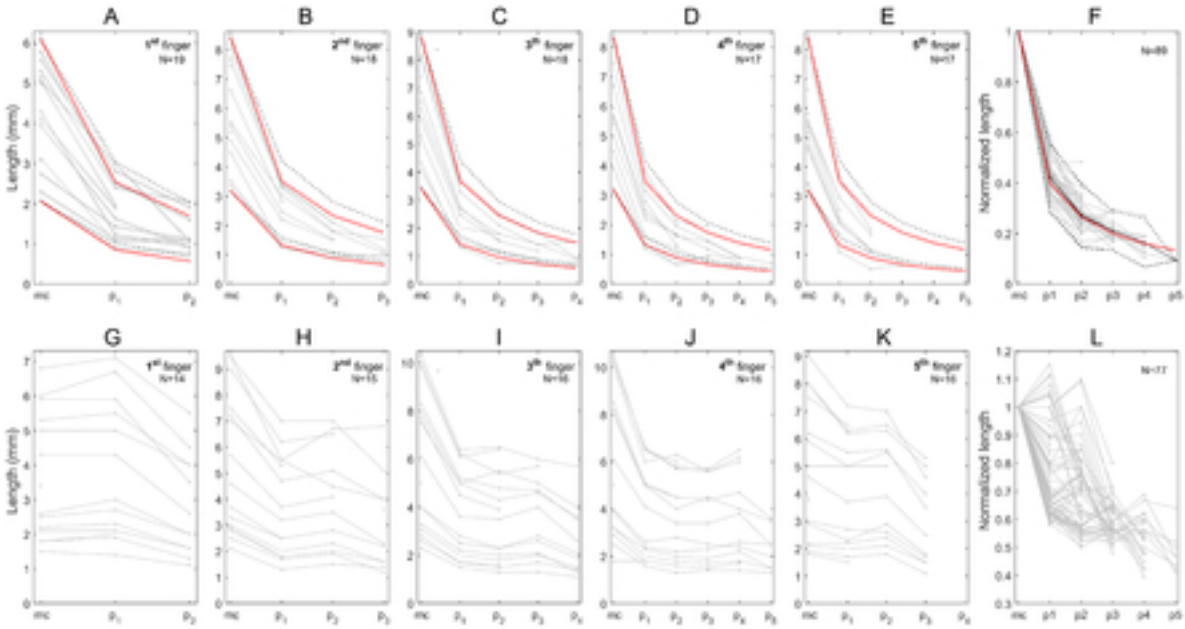

Figure 16. Metacarpal and phalanx lengths measured in each mesosaur finger (A-L). Black dashed lines represent the empirical curves pn=ct /(n+1) and red dotted lines represent the empirical curve px=ct /[(n+1)*1.2] for the largest and smallest measured finger, where ct is the length of the metacarpals and pn is the length of the n-th phalanx. (F) Shows the same information as (A-E), but lengths are normalized by the respective metacarpal length in all the measured fingers. Black line shows the mean normalized length; black dashed lines represent the 2σ interval. Red dotted line represents the empirical curve pn=ct /[(n+1)*1.2]. (G-K) Metacarpal and phalanx lengths measured in each Hovasaurus finger. (L) Lengths of all fingers normalized by the respective metacarpal length. The number of individuals measured (N) is indicated in the upper corner of each graph. ct – metatarsals, p1-p5 phalanges.

Figure 17

Download source file (927.85 kB)

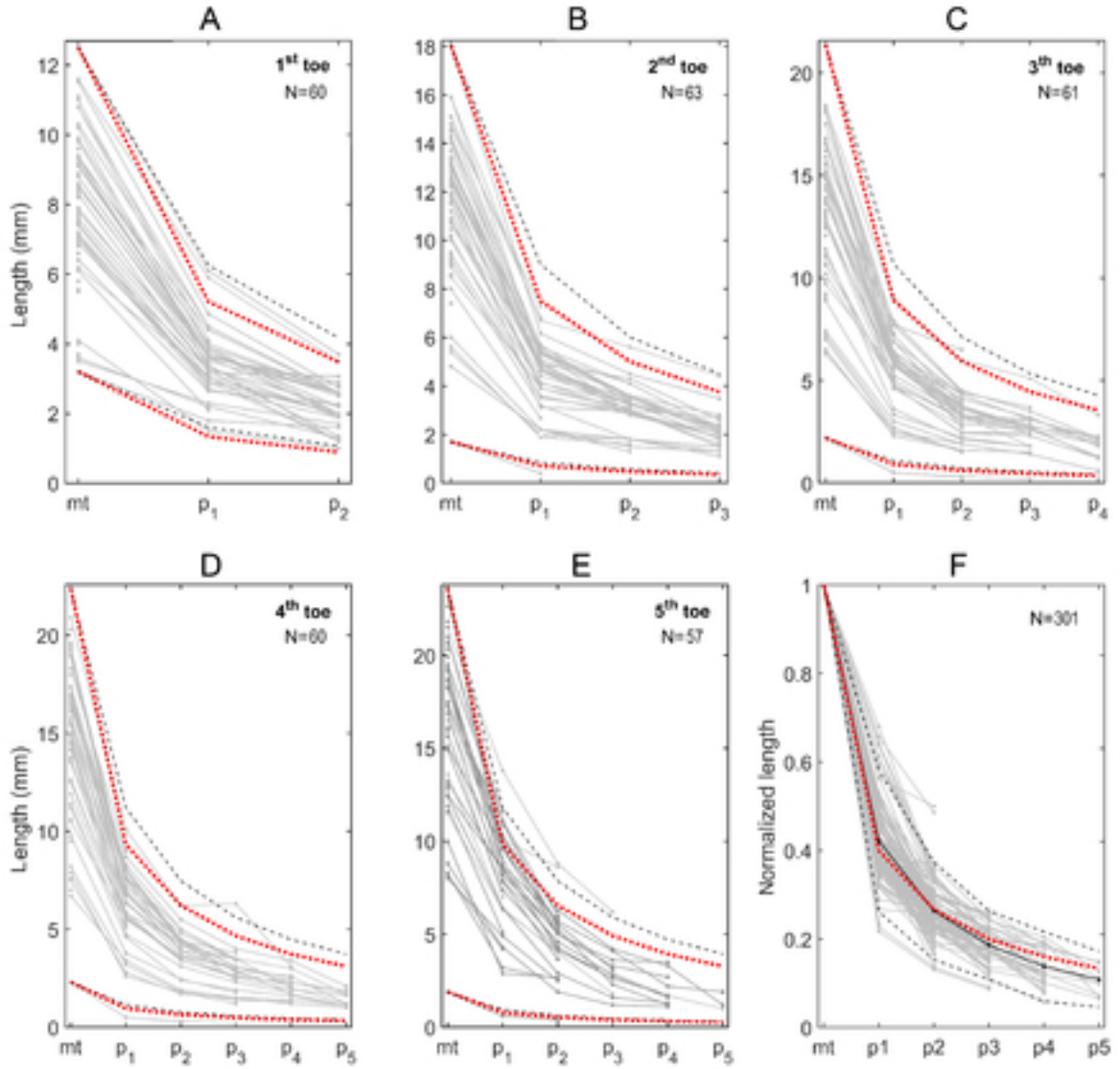

Figure 17. Metatarsal and phalanx lengths measured in each mesosaur toe (A-F). Black dashed line represents the empirical curves pn=mt /(n+1) and red dotted lines represent the empirical curve pn=mt /[(n+1)*1.2] for the largest and smallest measured toe, where mt is the length of the metatarsal and pn is the length of the n-th phalanx. (F) Shows the same information as (A-E), but lengths are normalized by the metatarsal length for all the measured toes. Black line shows the mean normalized length, black dashed lines represent the 2σ interval. Red dotted line represents the empirical curve pn=mt /[(n+1)*1.2]. The number of individuals measured (N) is indicated in the upper corner of each graph. mt – metatarsals, p1-p5 phalanges.

Figure 18

Download source file (165.43 kB)

ACTA PALAEONTOLOGICA POLONICA

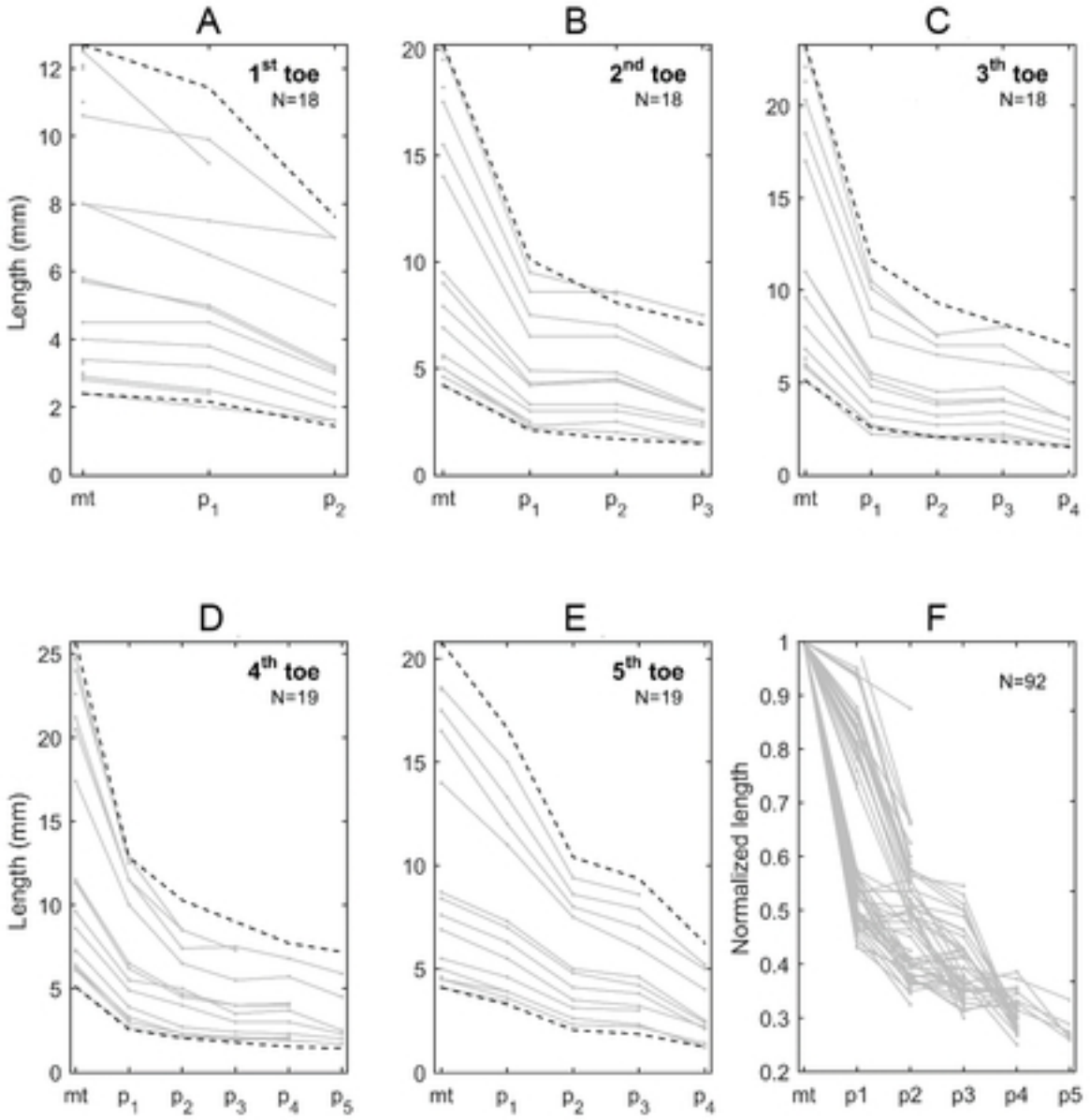

Figure 18. Metatarsal and phalanx lengths measured in each Hovasaurus toe (A-F). Black dashed line represents the empirical proportion for the longest and shortest measured toes described in the text. (F) shows the length after being normalized by the metatarsal length for all the measured toes. The number of individuals measured (N) is indicated in the upper corner of each graph. Mt: metatarsals, p1-p5: phalanges. Black dashed lines follow the empirical proportions described in the text.

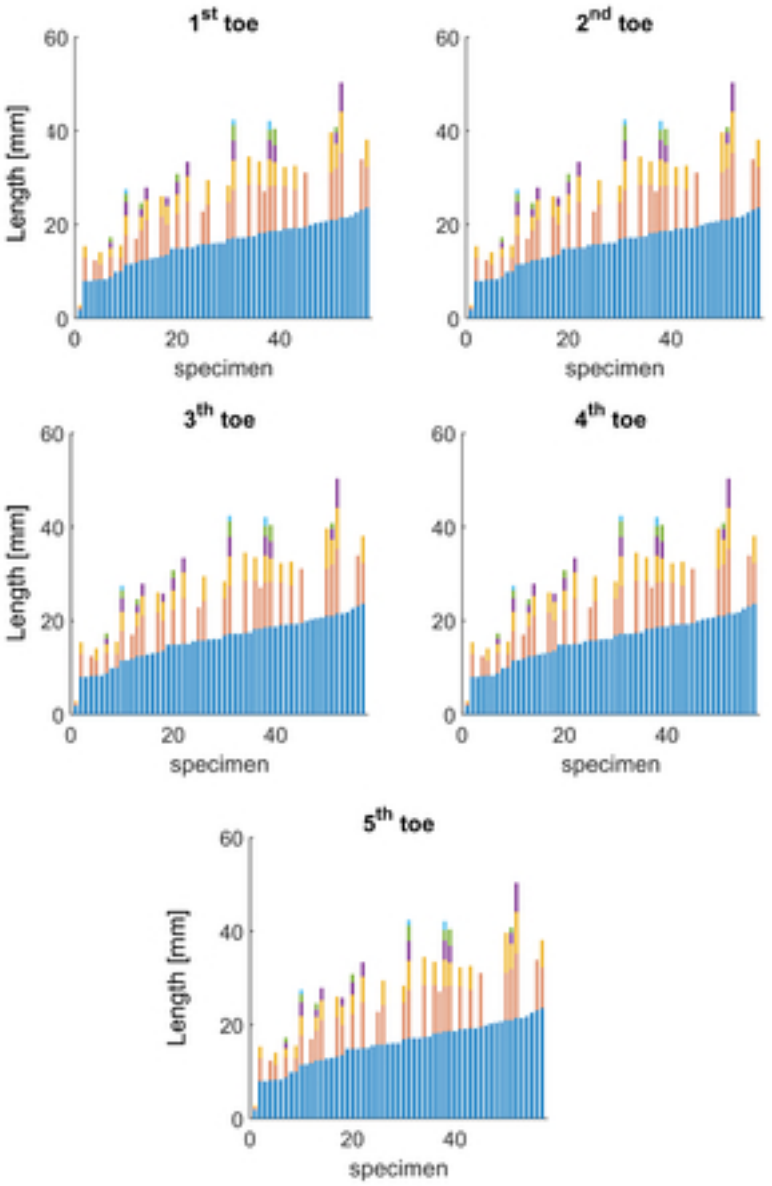

Figure 19. Stacked bar diagram of the mesosaur digits analysed, arranged by metatarsal size. Each bar represents the metatarsal and phalanx length measured in each specimen. First specimen in the plots is the unborn mesosaur specimen (FC-DPV 2504, Piñeiro et al. 2012a).

Figure 20

Download source file (656.46 kB)

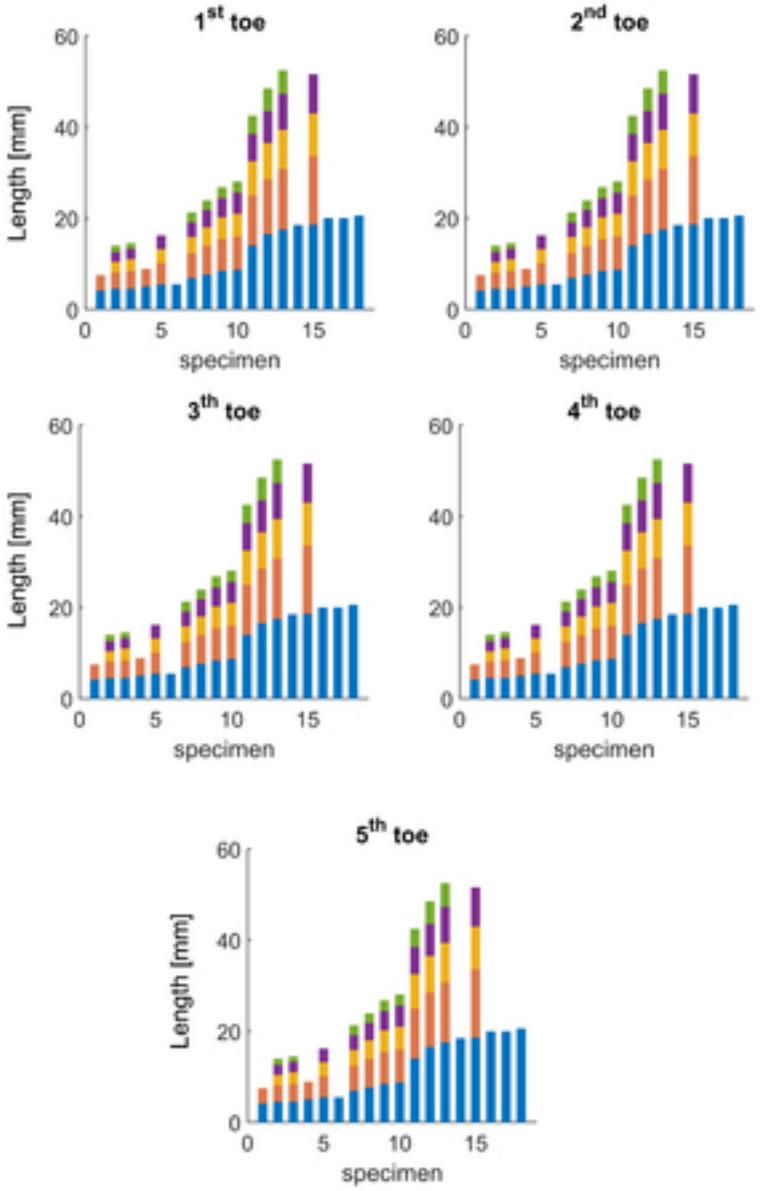

Figure 20. Stacked bar diagram of Hovasaurus digits analysed and arranged by metatarsal size. Each bar represents the metatarsal and phalanx length measured in each specimen.

Figure 21

Download source file (1.42 MB)

ACTA PALAEONTOLOGICA POLONICA

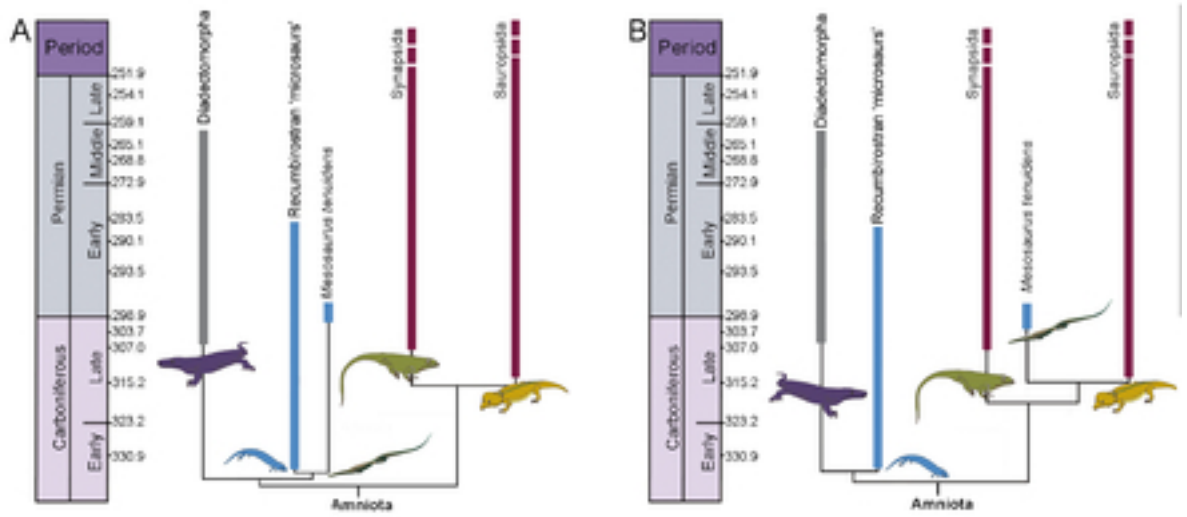

Figure 21. Calibrated position of mesosaurs regarding the pattern of growth known for the groups represented. Light blue bars represent taxa with isometric growth; dark purple bars represent those groups where allometric growth is the dominant pattern and medium grey bars are the groups where we do not have enough information to infer a growth pattern. A: Topology that suggest isometry as the most probable pattern for earliest amniotes. B: Topology that suggest that isometric growth pattern has been independently developed by recumbirostran ‘microsaurs’ and mesosaurs. Simplified phylogenies of basal amniotes were based on hypotheses from Carroll, (1995); Berman, (2000); Olori, (2015); Piñeiro et al, (2015); Liu and Beves, (2015); Laurin and Piñeiro (2017); Pardo et al, (2017). Chronostratigraphy is based on the 2018 Chart of the International Commission on Stratigraphy.

ACTA PALAEONTOLOGICA POLONICA

Manuscript body

File 1 - Download source file (115.48 kB)

Tables

Table 1 - Download source file (13.88 kB)

Table 2 - Download source file (10.91 kB)

Figures

Figure 1 - Download source file (922.87 kB)
Figure 1. Anatomical reconstruction of (A) pes / hindlimb and (B) manus / forelimb in an adult Mesosaurus tenuidens. Colours indicate the identity of the different elements that form the limbs. Scale bar: 10 mm. (CL?): Lateral Centrale? (ontogenetic development of this bone is discussed in detail in the carpus section), i-v finger/toe numbers. Modified from Piñeiro et al. (2016).

Figure 2 - Download source file (950.23 kB)
Figure 2. Anatomical reconstruction of (A) pes / hindlimb and (B) manus / forelimb in an adult Hovasaurus boulei. Colours indicate the identity of the different elements that form the limbs. i-v finger/toe number. Scale bar: 10 mm. Based in Currie (1981) and Caldwell (1997).

Figure 3 - Download source file (774.55 kB)
Figure 3. Relationships found in different regions of the mesosaur skull. (A-F) linear relationships between different elements of the mesosaur skull. (B): skull length against snout length (circles); skull length against “skull length minus snout length” (squares) PBO-PBS: length between the posterior border of orbit and the posterior border of the skull. The measured regions are indicated in the upper left corner of each figure; x and y indicate the axis on which the measurement is plotted. (G-I) shows the respective statistical parameters: (G) Coefficient a and its 95% confidence interval, (H) Correlation coefficient. (I) Number of samples.

Figure 4 - Download source file (181.25 kB)
Figure 4. Resultant parameters from the comparison between length and width of different limb bones of Mesosaurus. (A) Coefficient a and its 95% confidence interval, (B) Correlation coefficient. (C) Number of measurements/samples (squares) and number of individuals (diamonds) studied. Acronyms: l: length, pw: proximal width, cw: central width, dw: distal width.

Figure 5 - Download source file (1.3 MB)
Figure 5. Length vs. width relationships in different forelimb bones of mesosaurs. A-C. The measured bone and the measurements taken are indicated in the upper left corner of each figure (see Fig. 1). Proximal (+), medial (x) and distal (o) bone width. The statistical parameters are indicated in Fig. 4.

Figure 6 - Download source file (2.76 MB)
Figure 6. Length vs. width relationships in different hindlimb bones of mesosaurs. A-E. The measured bone and the measurements taken are indicated in the upper left corner of each figure (see Fig. 1). Proximal (+), medial (x) and distal (o) bone width. Statistical parameters are indicated in Fig. 4.

Figure 7 - Download source file (174.3 kB)
Figure 7. Resultant parameters from comparison between the length of different mesosaur limb bones. (A): Coefficient a and its 95% confidence interval. (B): Correlation coefficient. (C): Number of measurements/samples (squares) and number of individuals (diamonds) studied. Acronyms: As: Astragalus, CI-CV: Metacarpals, Fe: Femur, Fi: Fibula, Hu: Humerus, Ra: Radius, Ti: Tibia, TI-TV: Metatarsals, Ul: Ulna.

Figure 8 - Download source file (1.69 MB)
Relationship between the lengths of different mesosaur forelimb and hindlimb bones. The respective statistical parameters are provided in Fig. 7. CI-CV: Metacarpals, TI-TV: Metatarsals.

ACTA PALAEONTOLOGICA POLONICA

Figure 9 - Download source file (2.82 MB)
Figure 9. Lengths of femora vs. zeugopodia in mesosaurs. Blue plus signs: fibulae measurements; Red circles: tibiae measurements. Statistical parameters are shown in Fig. 7. A-T: Tarsal ontogeny of embryonic to adult mesosaurs illustrated following Piñeiro et al. (2016), see also Fig. 12. A: FC-DPV 2504; B:AMNH 23799; C:SMF-R4513-young; D: GP-2E 272; E: AMNH 23795; F: SMF-R 4496; G: SMF-R 4513-older; H: SMF-R 4934; I: MN 4741; J:PIMUZ A-III 591; K: GP-2E 114; L:GP/2E 6519-E; N: GP/2E 6519-A; O: SMF-R 4470; P: SMF-R 4528; Q: GP-2E 657b; R: FC-DPV 2058; S: GP-2E 5740; T:SMF-R 4477. Specimens A, D-I, K, M, O-S were previously analysed by Piñeiro et al. (2016).

Figure 10 - Download source file (1.86 MB)
Figure 10. Relationships between skull length, vertebral mean length and stylopodium length in mesosaurs. (A): Relationship between skull length and vertebral mean length. Ontogenetic stage of the specimens is illustrated following Piñeiro et al. (2016), see also Fig. 12. B:AMNH 23799; C:SMF-R4513-young; H: SMF-R 4934; J:PIMUZ A-III 591; L:GP/2E 6519-E; M: PF IPL 220011/04 770; N: GP/2E 6519-A; P: SMF-R 4528; Specimens H, M, P were previously analysed by Piñeiro et al. (2016). (B): Relationship between femur length and vertebral mean length with its 3σ interval. (C): Relationship between skull length, and zeugopodial length in mesosaurs. 95% confidence interval is shown in each plot.

Figure 11 - Download source file (8.22 MB)
Figure 11. Structure of the mesosaur carpus in presumed subadult and adult specimens. (A-B): Photographs and interpretive drawings of manus of sub-adult or young adult mesosaur specimens (SMF-R 4492 and 4528 respectively). In B, five bones can be seen in the proximal carpal series, including a small ossified radiale close to the lateral centrale. Four bones (and perhaps an incipiently ossified very small distal V) are preserved in the distal series. (C1-C2):, Interpretive drawings and photographs of right and left manus respectively of SMF-R 4710, a more mature specimen, which has only three bones in the proximal series, after the fusion of radiale, lateral centrale, and probably the medial centrale. There are five bones in the distal series, but the fifth continue to be the smallest. A small pisiforme can be seen in (C2). (D1-D2): Interpretive drawings and photographs of left and right manus of MNHN AC 1865-77A, the type specimen of Mesosaurus tenuidens Gervais, 1865, a mature mesosaur specimen showing the incipient fusion of intermedium and centralia plus radiale complex. A pisiforme and a distal tarsal V could have been present but were lost or are not well-preserved. Abbreviations: lc. lateral centrale; mc. medial centrale; i. intermedium; pis, pisiform; rl, radiale; ra, radius, ul, ulna; ur, ulnare. Scale bars: 5 mm.

Figure 12 - Download source file (1.48 MB)
Figure 12. Variation of the mesosaur carpus structure through the growth. (A1-A2): Interpretive drawing of SMF-R 4485, left and right manus of a very immature individual, where just three rounded, featureless bones (intermedium, ulnare and possible lateral centrale) are present in the carpus. (B): Interpretive drawing of SMF-R 4528, specimen showing the most common carpus structure found in the available materials, where the intermedium and the centralia complex place closer together to finally fuse each other. A small radiale is still present (in light blue color). (C1-C2): Interpretive drawing of MCN-PV 2238A and B, part and counterpart of left manus showing the radiale (in light blue color) close to completing its fusion to the centralia. (D): Interpretive drawing of MN 7148 showing a more mature carpus and a small possible pisiforme (in dark red) present close to the ulnare carpal bone. (E1-E2): Interpretive drawing of SMF-R 4710, right and left manus of an adult mesosaur with the intermedium and the centralia plus radiale complex yet not fused. A small possible pisiform (in dark red) is present only in the right manus and absent from the left. (F1-F2): Interpretive drawing of MNHN AC 1865-77A, partial right and left forelimbs and manus of the type specimen of Mesosaurus tenuidens Gervais, 1865, where an incipient fusion of the intermedium with the centralia plus radial complex can be observed. There seem to be five distal tarsals although the fifth is indeed very small. Also, there can be a pisiforme, but the hands in this specimen have been exposed to partial degradation by the action of scavengers that damaged some of the smallest bones. Scale bars: 10 mm.

Figure 13 - Download source file (5.46 MB)
Figure 13. Mesosaurus tenuidens, ontogenetic transformation in the tarsus formation (after Piñeiro et al. 2016). A-T: Drawings of the selected specimens preserving epipodial, mesopodial and metapodial elements. SA: FC-DPV 2504; B:AMNH 23799; C:SMF-R4513-young; D: GP-2E 272; E: AMNH 23795; F: SMF-R 4496; G: SMF-R 4513-older; H: SMF-R 4934; I: MN 4741; J:PIMUZ A-III 591; K: GP-2E 114; L:GP/2E 6519-E; M: PF IPL 220011/04 770; N: GP/2E 6519-A; O: SMF-R 4470; P: SMF-R 4528; Q: GP-2E 657b; R: FC-DPV 2058; S: GP-2E 5740; T:SMF-R 4477. Specimens A, D-I, K, M, O-S were previously analysed by Piñeiro et al. (2016).

Figure 14 - Download source file (679.09 kB)
Figure 14. Schematic diagram of the ontogenetic transformation of the Mesosaurus tenuidens tarsus. Five stages are divided according to the ossification of the astragalus, calcaneum and navicular. Distal tarsal morphology can display some variations regarding the degree of ossification of the constituent bones (see the text). The approximate sizes (in millimetres) that the different elements would have in the transition between each category are tabulated according to our observations.

Figure 15 - Download source file (3 MB)
Figure 15. Metacarpal length measured in each Mesosaurus (A) and Hovasaurus (B) manus. Metatarsal lengths measured in each mesosaur (C) and Hovasaurus (D) pes. Each line represents the hand or foot of one specimen. Number of samples (N) is shown in each figure. Black dotted line represents the empirical proportions followed for the mesosaur metatarsals: mt(n)=mt(1)+n/4 where mt(1) is the measure of the first metatarsal. Metapodium is represented in the upper left corner of each figure (see Figs. 1, 2).

Figure 16 - Download source file (3.22 MB)
Figure 16. Metacarpal and phalanx lengths measured in each mesosaur finger (A-L). Black dashed lines represent the empirical curves pn=ct /(n+1) and red dotted lines represent the empirical curve px=ct /[(n+1)*1.2] for the largest and smallest measured finger, where ct is the length of the metacarpals and pn is the length of the n-th phalanx. (F) Shows the same information as (A-E), but lengths are normalized by the respective metacarpal length in all the measured fingers. Black line shows the mean normalized length; black dashed lines represent the 2σ interval. Red dotted line represents the empirical curve pn=ct /[(n+1)*1.2]. (G-K) Metacarpal and phalanx lengths measured in each Hovasaurus finger. (L) Lengths of all fingers normalized by the respective metacarpal length. The number of individuals measured (N) is indicated in the upper corner of each graph. ct – metatarsals, p1-p5 phalanges.

Figure 17 - Download source file (927.85 kB)
Figure 17. Metatarsal and phalanx lengths measured in each mesosaur toe (A-F). Black dashed line represents the empirical curves pn=mt /(n+1) and red dotted lines represent the empirical curve pn=mt /[(n+1)*1.2] for the largest and smallest measured toe, where mt is the length of the metatarsal and pn is the length of the n-th phalanx. (F) Shows the same information as (A-E), but lengths are normalized by the metatarsal length for all the measured toes. Black line shows the mean normalized length, black dashed lines represent the 2σ interval. Red dotted line represents the empirical curve pn=mt /[(n+1)*1.2]. The number of individuals measured (N) is indicated in the upper corner of each graph. mt – metatarsals, p1-p5 phalanges.

Figure 18 - Download source file (165.43 kB)
Figure 18. Metatarsal and phalanx lengths measured in each Hovasaurus toe (A-F). Black dashed line represents the empirical proportion for the longest and shortest measured toes described in the text. (F) shows the length after being normalized by the metatarsal length for all the measured toes. The number of individuals measured (N) is indicated in the upper corner of each graph. Mt: metatarsals, p1-p5: phalanges. Black dashed lines follow the empirical proportions described in the text.

Figure 19 - Download source file (756.28 kB)

Figure 19. Stacked bar diagram of the mesosaur digits analysed, arranged by metatarsal size. Each bar represents the metatarsal and phalanx length measured in each specimen. First specimen in the plots is the unborn mesosaur specimen (FC-DPV 2504, Piñeiro et al. 2012a).

Figure 20 - Download source file (656.46 kB)
Figure 20. Stacked bar diagram of Hovasaurus digits analysed and arranged by metatarsal size. Each bar represents the metatarsal and phalanx length measured in each specimen.

Figure 21 - Download source file (1.42 MB)
Figure 21. Calibrated position of mesosaurs regarding the pattern of growth known for the groups represented. Light blue bars represent taxa with isometric growth; dark purple bars represent those groups where allometric growth is the dominant pattern and medium grey bars are the groups where we do not have enough information to infer a growth pattern. A: Topology that suggest isometry as the most probable pattern for earliest amniotes. B: Topology that suggest that isometric growth pattern has been independently developed by recumbirostran 'microsaurs' and mesosaurs. Simplified phylogenies of basal amniotes were based on hypotheses from Carroll, (1995); Berman, (2000); Olori, (2015); Piñeiro et al, (2015); Liu and Beves, (2015); Laurin and Piñeiro (2017); Pardo et al, (2017). Chronostratigraphy is based on the 2018 Chart of the International Commission on Stratigraphy.

Supplementary Online Material

File 1 - Download source file (19.78 kB)